Supplementary Information for:

Stability of Adsorbents for Direct Air Capture (DAC): Challenges and Perspectives

Salar Fakhraddinfakhriazar[a], *Cristhian Molina-Fernández*[a] and *Grégoire Léonard*[a*]

[a] Department of Chemical Engineering, Université de Liège, B37 Sart-Tilman, 4000 Liège, Belgium

[*] G.Leonard@uliege.be

Table of Content of Supplementary Information

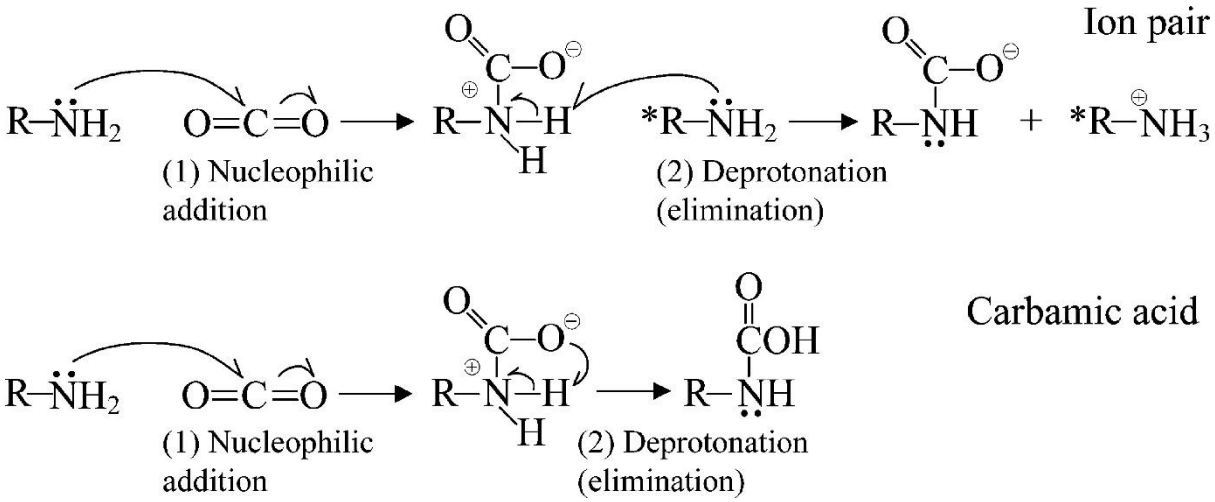

Scheme S1. Reaction pathways for CO_2 capture by primary amines. Reproduced with permission from ref 1. Copyright 2014 American Chemical Society.

In this reaction, the nitrogen atom of the amine functional group (R-NH_2) acts as a Lewis base, donating its lone pair electrons to selectively and reversibly bind CO_2, which functions as a Lewis acid. The nucleophilic nitrogen attacks the electrophilic carbon center of CO_2, forming a zwitterionic intermediate that subsequently reacts with adjacent amine groups to yield ammonium carbamate and/or carbamic acid. In the presence of water, sterically hindered amines preferentially form bicarbonate species.[2]

Impregnation: In this method, after dissolving amine material in organic solvent (e.g., methanol or ethanol) or water while stirring, the required amount of support material (e.g., silica) is added to the amine solution, followed by stirring to disperse amine component into the pores of the support. Finally, the solution is filtered, and the solvent is removed either under vacuum or by heating up in oven.[3] Examples of aminopolymers used for the preparation of amine-impregnated DAC adsorbents include poly(ethylenimine) (PEI), poly(propylene imine) (PPI), poly(propylene guanidine) (PPG), poly(allylamine) (PAA), and poly(glycidyl amine) (PGA). The impregnation of smaller amine molecules such as tetraethylenepentamine (TEPA), triethylenetetramine (TETA), pentaethylenehexamine (PEHA), tris(2-aminoethyl)amine (TREN), diethylenetriamine (DETA), and ethylenediamine (ED) are also examined in the literature. The chemical structure of these amine components is illustrated in Chart S1 and Chart S2.

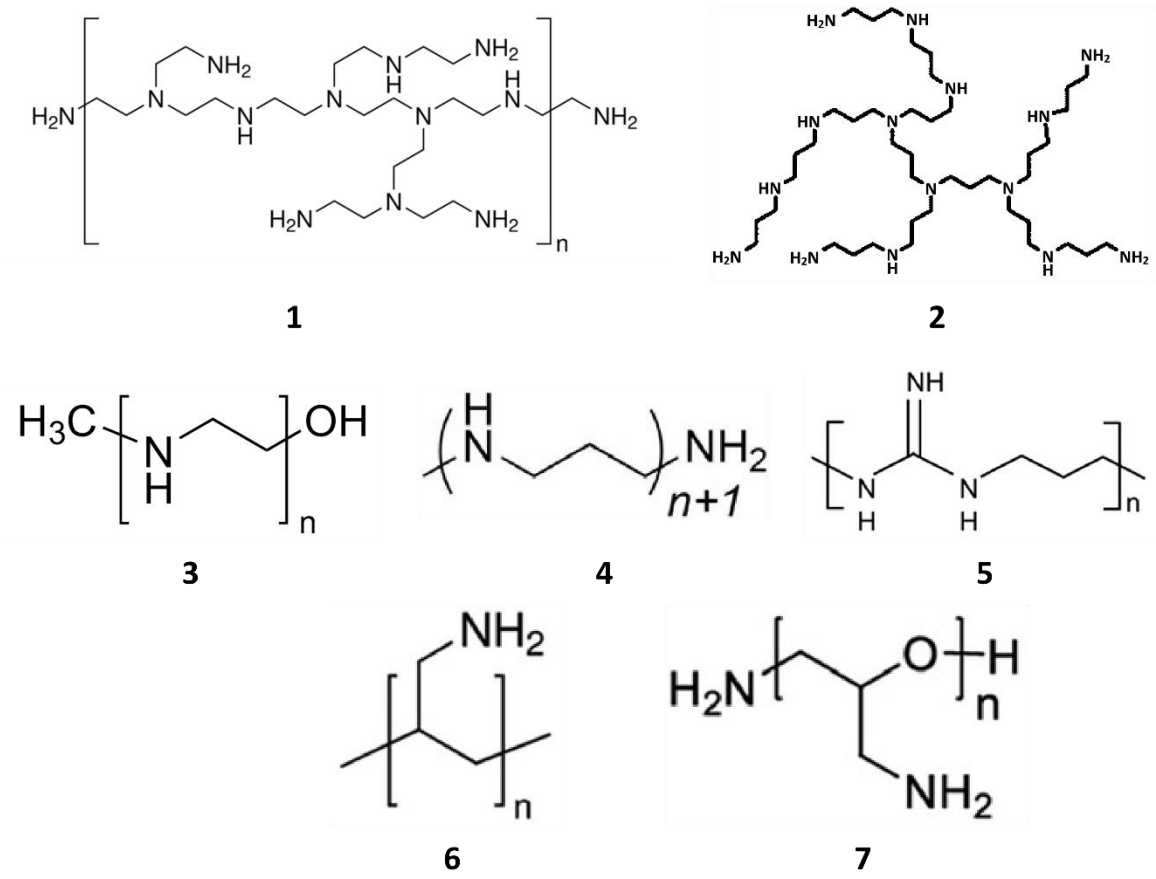

Chart S1. Chemical structure of aminopolymers used for impregnation: branched poly(ethylenimine) (bPEI), branched poly(propylene imine) (bPPI),[4] linear poly(ethylenimine) (lPEI), linear poly(propylene imine) (lPPI),[5,6] poly(propylene guanidine) (PPG),[7] poly(allylamine) (PAA),[8–10] and poly(glycidyl amine) (PGA),[11] respectively.

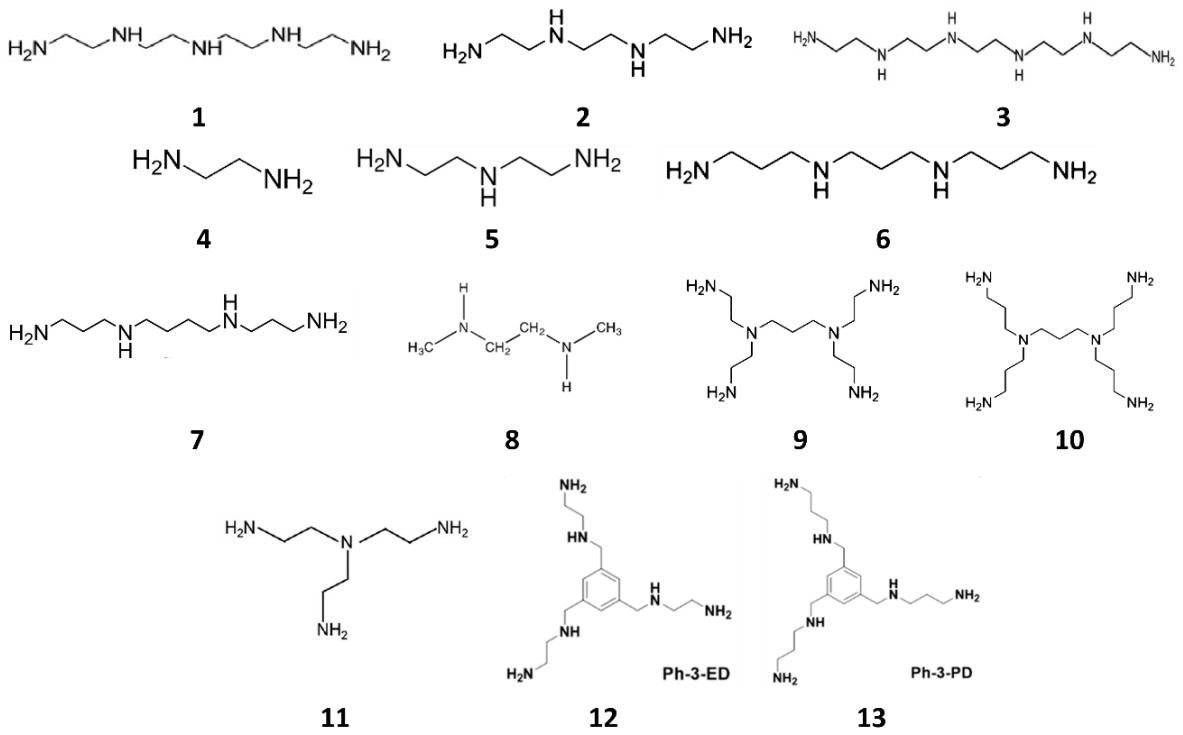

Chart S2. Chemical structure of amines used for impregnation: tetraethylenepentamine (TEPA), triethylenetetramine (TETA),[12–14] pentaethylenehexamine (PEHA),[13,15,16] ethylenediamine (ED),[16,17] diethylenetriamine (DETA),[16] tripropylenetetramine (TPTA),[14] spermine (SPER),[13] N,N'-Dimethylethylenediamine (DMEDA),[18] dendritic PEI (EI-den),[14] dendritic PPI (PI-den),[14] tris(2-aminoethyl)amine (TREN),[19] aromatic core with ethylenediamine,[20] and aromatic core with propylenediamine,[20] respectively.

PEI has been extendedly used for impregnation due to its availability, low cost, ease of customization, and high amine content. While smaller PEI molecules can diffuse more uniformly into the pores of the support, larger molecules show better regeneration stability under humid conditions thanks to lower water solubility.[21] This aminopolymer is available in both branched (bPEI) and linear structures (lPEI). The capture capacity of lPEI is slightly lower than bPEI. The latter has been more commonly used in the literature for the synthesis of solid adsorbents due to its lower cost and greater availability.[22] Regarding the type of amine groups, bPEI is composed of primary, secondary, and tertiary amines, with their CO_2 adsorption effectiveness being highest for primary, followed by secondary and tertiary.[23] While lPEI is mostly composed of secondary amines, bPEI has a higher proportion of primary amines at the ends of its backbones. Tertiary amines are usually created at the branching points within the chain, especially in dendrimer structures.[24] Unlike primary and secondary amines that are capable of capturing CO_2 under dry and humid conditions, tertiary amines capture CO_2 only in presence of humidity..[23] Furthermore, tertiary amines are not effective in the adsorption of CO_2 due to the slow ammonium bicarbonates formation.[25,26] Therefore, to ensure high amine efficiency of amine-based adsorbents, the Mw and amine type ratio need to be adjusted appropriately.

PPI, with three methylene groups in the monomer, is another aminopolymer used for impregnation on porous solid that can present linear, branched, or dendritic forms.[14] Even though PPI-based adsorbents were reported to have higher capture capacity than PEI-impregnated samples,[5,14] their application is limited by the complicated monomer synthesis and slow polymerization process.[24] PAA with dense primary amines in its structure has been also impregnated on porous support.[27]

Besides aminopolymers, other amine molecules were used for impregnation. TEPA, for instance, has been extensively studied in the literature owing to its high sorption capacity. TEPA with five amine groups can theoretically capture a maximum of five CO_2 molecules per molecule.[21] TEPA and BPEIs contain 40 mol% and 42–44 mol% primary amines with respect to the total amine groups, respectively.[11,28,29] Likewise, other amines like TETA and PEHA were also appropriate for impregnation exhibiting similar capture capacity.[16] In comparison to TEPA, PEHA has an additional amine group in its structure and demonstrates an acceptable CO_2 capacity.[15] TREN is a promising amine for CO_2 capture as it is a small amine presenting a high density of primary amines.[19]

Grafting: In the process of synthesizing grafted adsorbents, the required amount of porous solid support is added to a solvent, generally anhydrous toluene, with continuous stirring. Subsequently, aminosilane is added to the solution while keeping the stirring and conducting reflux. Finally, the solution is filtered and washed to remove the remaining unreacted amine.[30] Among various grafted aminosilanes, the performance of (3-aminopropyl)triethoxysilane (APTES), 3-(aminopropyl)trimethoxysilane (APTMS), 3-(2-aminoethylamino)propyltrimethoxysilane (DI), and 3-[2-(2-aminoethylamino)ethylamino]propyltrimethoxysilane (TRI) grafted sorbents are extensively assessed in the literature. The chemical structure of these aminosilanes is illustrated in Chart S3.

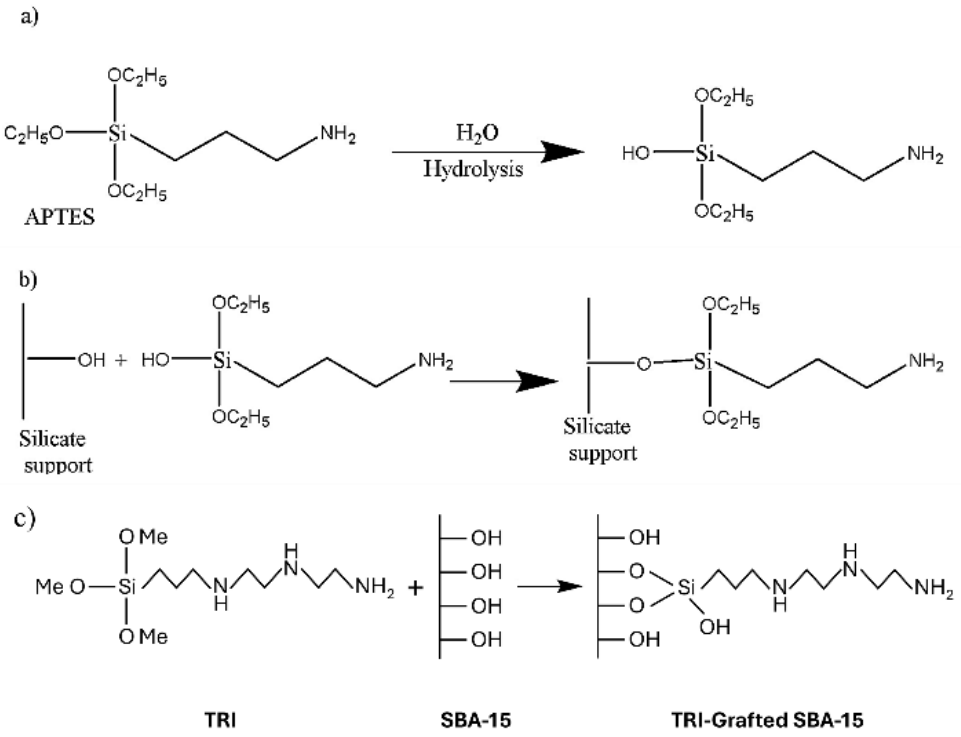

Scheme S2. Reactions occurring during APTES grafting on silica in the presence of water: (a) APTES hydrolysis and (b) the reaction between silanol intermediates (Si-OH) and the hydroxyl groups on the silica surface; adapted from; (c) grafting TRI on SBA-15. Reproduced with permission from ref 31. Copyright 2018 Elsevier Publication.

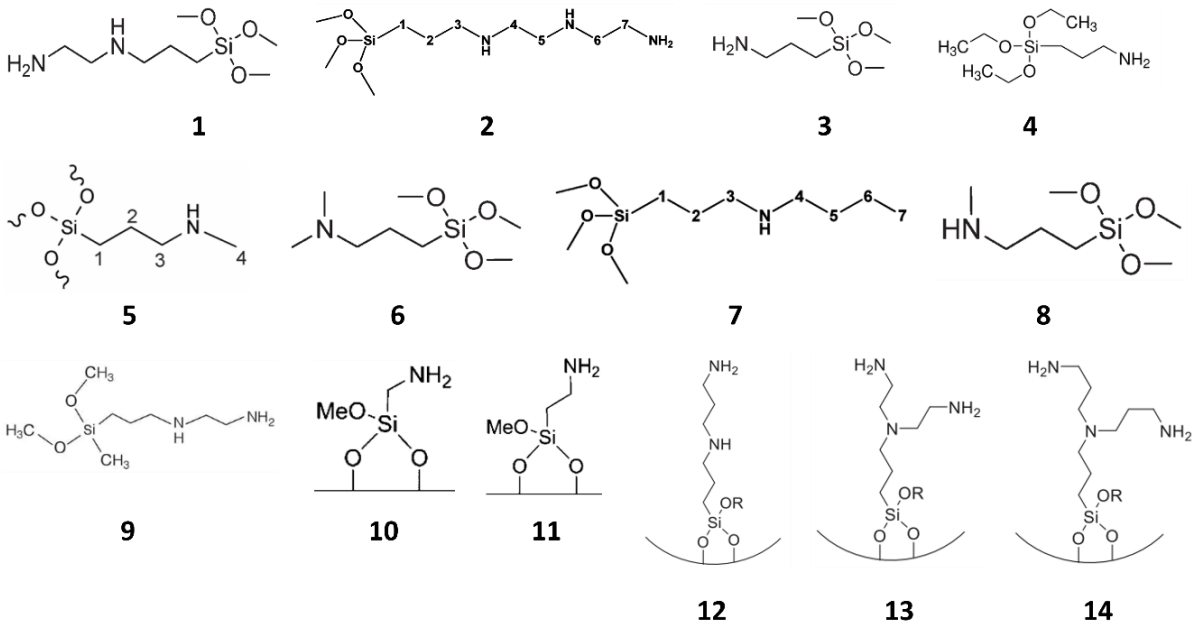

Chart S3. The chemical structure of aminosilanes used in the literature for synthesizing amine-grafted DAC adsorbents N-[3-(trimethoxysilyl)propyl]ethylenediamine or 3-(2-aminoethylamino)propyltrimethoxysilane (DI),[8,32–35] N^1-(3-trimethoxysilylpropyl)diethylenetriamine or 3-[2-(2-aminoethylamino)ethylamino]propyltrimethoxysilane or 2-[2-(3-trimethoxysilylpropylamino) ethylamino]ethylamine (TRI),[8,32,36–41] 3-(trimethoxysilyl)propylamine or 3-(aminopropyl)trimethoxysilane (APTMS),[42] (3-aminopropyl)triethoxysilane (APTES),[43] trimethoxy[3-(methylamino)propyl]silane or N-methylaminoproyltrimethoxysilane (TMMAPS),[42] (N,N-dimethylaminopropyl)trimethoxysilane (DMAPS),[33] N-butylaminopropyl trimethoxysilane,[8] (N-methylaminopropyl)-trimethoxysilane or (3-methylaminopropyl)trimethoxysilan (MAPS),[33] N-(2-aminoethyl)-3-aminopropylmethyldimethoxysilane (AEAPDMS),[44] aminomethyltriethoxysilane,[45] 2-aminoethyltrimethoxysilane,[45] 3-(2-aminopropylamino)propyltrimethoxysilane (L-propyl),[34] N^1-(2-Aminoethyl)-N^1-(3-(triethoxysilyl)-propyl)ethane-1,2-diamine (B-ethyl),[34] N^1-(3-Aminopropyl)-N^1-(3-(triethoxysilyl)propyl)propane-1,3-diamine (B-propyl),[34] respectively.

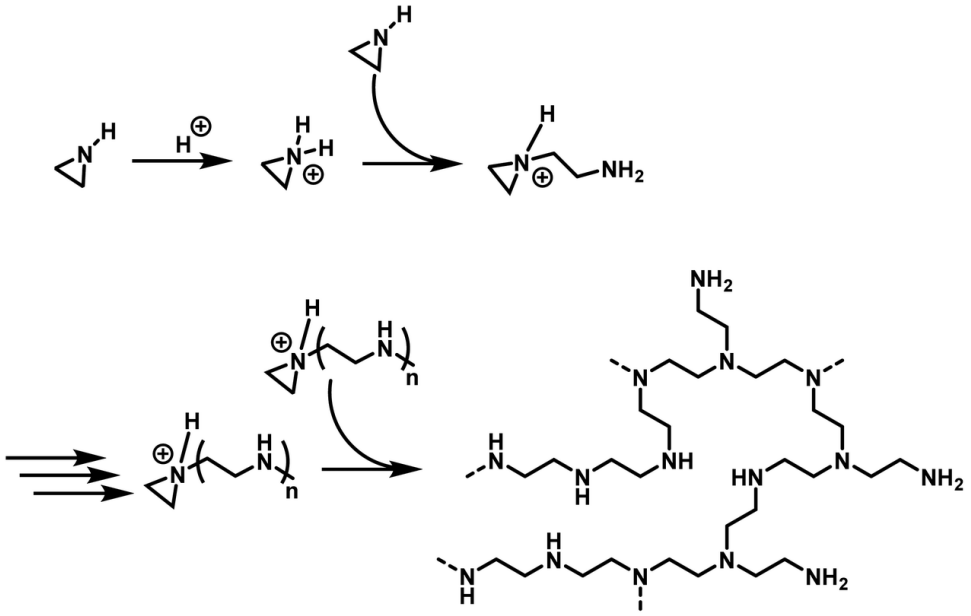

Scheme S3. Cationic ring-opening polymerization pathway of aziridine for BPEI synthesis. Reproduced with permission from ref 46. Available under a CC-BY license. Copyright 2019 Gleede et al.

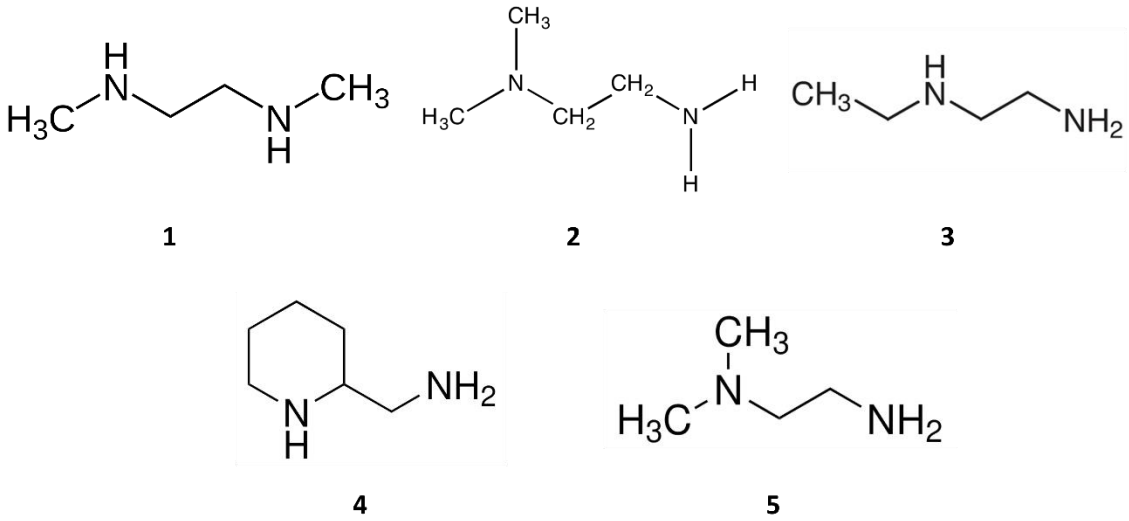

Chart S4. Structure of amines post-synthetically appended to MOFs N,N′-dimethylethylenediamine (DMEDA, "mmen"),[47] 1,1-dimethylethylenediamine (den),[48] N-ethylethylenediamine (een),[49] 2-(aminomethyl)piperidine (2-ampd),[50] N,N-dimethylethylenediamine (mm-2),[51] respectively.

The summary tables present key details from cited studies in a structured format:

- The first column lists the main author(s) and the publication year.
- The second column specifies the tested adsorbent(s), followed by information on the support material and active component used in the solid sorbent. The molecular weight (Mw) of the amine component is provided in parentheses if defined in the reference article, along with the synthesis method.
- Active component loading is provided, typically expressed as weight percentage (mass of amine/mass of support), unless stated otherwise.
- The experimental mode is categorized as either continuous exposure (C.E.) or cyclic. For cyclic tests, the regeneration type (e.g., TSA, TVSA, etc.) is specified in parentheses.
- If experiments were conducted using a TGA device or gravimetric analysis, “G.A.” is noted, whereas “P.B.” is used for packed bed column experiments.
- For continuous experiments, experimental conditions are summarized.
- In cyclic tests, the number of cycles is followed by the conditions of the adsorption step (left column) and regeneration step (right column).
- Adsorption and regeneration conditions include test gas composition (with the balance gas indicated last), dry (D) or humid (H) stream, adsorption/regeneration temperature(s), pressure, gas flow rate, relative humidity of the test gas, and adsorption/regeneration duration.
- Finally, the last column provides a summary of the main findings from each cited study.

Sample Table

Reference	**Adsorbent**	**Support material**	**Active Component**	**Loading**	**Mode of Experiment**		**Thermal/Oxidative/Hydro(thermal) stability**		**Remarks**
							Adsorption	**Regeneration**	
Main Author(s) (year of publication) [reference]	Name of studied adsorbent (1)	Type of support material (e.g., silica, alumina, etc.)	Active capture component 1 (Mw) (synthesis method)	in wt% unless specified	Cyclic Or continuous exposure (C.E.)	Gravimetric Analysis (G.A.) or Packed Bed (P.B.) experiment	Number of Cycles		• Main results are summarized.
							Test gas composition for adsorption (D) or (H) Adsorption temperature Adsorption pressure Relative humidity Gas flowrate (adsorption step duration)	Sweeping/regeneration gas composition (D) or (H) Desorption temperature Desorption pressure Relative humidity Gas flowrate (desorption step duration)	

Table S1. Summary of studies on the **thermal stability** of solid DAC adsorbents, including adsorbent types, experimental conditions, and key findings.

Reference	Adsorbent	Support material	Active Component	Loading (wt%)	Mode of Experiment		Thermal stability		Remarks
							Adsorption	Regeneration	
Abhilash et al. (2015)[52]	MAHSM	Polysilsesquioxane	APTES	≈ 50	Cyclic (TSA)	G.A.	100 cycles		• No capacity decrease was observed.
							CO_2 30 °C 100 mL/min (15 min)	He 80 °C 70 mL/min (15 min)	
							50 cycles		• No capacity loss was recoded under ambient air.
							Ambient air 30 °C 100 mL/min RH = 60% (100 min)	He 80 °C 70 mL/min (15 min)	
Alesi and Kitchin (2012)[53]	Lewatit VPOC1065	Polystyrene-divinylbenzene	Primary amine	N.A.	Cyclic (TSA)	G.A.	18 cycles		• Stable cyclic capacity of about 1.2 mmol/g.
							10% CO_2/N_2 (D) 50 °C 200 mL/min	N_2 120 °C 200 mL/min	
Anyanwu et al. (2020)[54]	W-AG-150	Silica gel	TRI (grafting)	5.12 $mmol_N/g$	Cyclic (TSA)	G.A.	17 cycles		• About 10% capacity loss.
							70% CO_2/He 75 °C	He 90 °C	
Anyanwu et al. (2022)[55]	WG-HBS-0.6	Hierarchical bimodal mesoporous silica	TRI (grafting)	≈ 48	Cyclic (TSA)	G.A.	10 cycles		• The CO_2 adsorption capacity was recorded after the initial 60 seconds of each adsorption cycle.
							70% CO_2/He 75 °C	He 90 °C	
Bali et al. (2015)[56]	AlK5	Alumina	Potassium acetate (impregnation)	5	Cyclic (TSA)	G.A.	5 cycles		• Stable capacity of 1.15 and 1.20 mmol/g regenerated at 250 and 350 °C, respectively. • Gradual capacity decline regenerated at 110 °C.
							1% CO_2/He 25 °C (3 h)	He 110, 250, 350 °C (3 h)	
	AlK10			10			5 cycles		• Stable cyclic uptake of 0.63 mmol/g over tested cycles.
							400 ppm CO_2/He 25 °C (3 h)	He 250 °C (3 h)	
							5 cycles		• Constant cyclic performance with final capacity of about 1.1 mmol/g.
							1% or 400 ppm CO_2/He 25 °C (3 h)	He 250 and 350 °C (3 h)	
							5 cycles		• Stable cyclic uptake of 0.67 mmol/g over tested cycles.
							1% or 400 ppm CO_2/He 25 °C (3 h)	He 250 °C (3 h)	

Reference	Adsorbent	Support material	Active Component	Loading (wt%)	Mode of Experiment		Thermal stability		Remarks
							Adsorption	Regeneration	
Cai et al. (2015)[57]	HNTs-PEI-30	Halloysite nanotubes	bPEI (Mw 17000) (impregnation)	30	Cyclic (TVSA)	G.A.	50 cycles Air (D) 25 °C 100 mL/min	80 °C 10^{-5} bar vacuum	• Slight uptake capacity decrease of the adsorbent.
					C.E.		TGA mass loss observed up to 600 °C.		• PEI started to decompose at 280 °C with maximum mass loss rate at 355 °C. • 50% total mass loss at 600 °C.
Chaikittisilp et al. (2011)[58]	SynA40	mesoporous γ-alumina	bPEI (Mw 800) (impregnation)	40	Cyclic (TSA)	G.A.	3 cycles 400 ppm CO_2/Ar (D) 25 °C 100 mL/min (12 h)	Ar (D) 110 °C 100 mL/min (3 h)	• Stable carbon capture capacity over 3 cycles.
	MS40	mesoporous silica SBA-15							
Chaikittisilp et al. (2011)[9]	PAA_MCF_41	Mesocellular Silica Foam (MCF)	PAA (impregnation)	41	Cyclic (TSA)	P.B.	3 cycles 10% CO_2/Ar (D) 25 °C 100 mL/min	Ar 110 °C 100 mL/min	• The CO_2 capacity was stable for both samples.
	PEIBr_MCF_39		BPEI, (Mw 800) (impregnation)	39					
Chao et al. (2013)[59]	TEPA/as-SBA- 15	SBA-15	TEPA (impregnation)	50	Cyclic (TVSA)	G.A.	10 cycles 15% CO_2/N_2 (D) 75 °C (1 h)	He 100 °C (1 h)	• Adsorbent with SBA-15 as support lost 20% capacity, whereas one with fumed silica support encountered 15% capacity decrease.
	TEPA/Fumed silica	Fumed silica							
Chen et al. (2013)[60]	HP20/PEI-50	HP20 resin	bPEI (Mn 600) (impregnation)	50	Cyclic (TSA)	P.B.	5 cycles 400 ppm CO_2/N_2 25 °C (12 h)	N_2 100 °C 100 mL/min (3 h)	• No significant capacity decrease after 5 cycles.
Chen et al. (2024) [61]	TRI-Al_2O_3	γ-alumina	TRI (grafting)	≈ 20	C.E.	G.A.	Weight loss observed up to 500 °C		• Bare alumina exhibited degradation between 200 and 240 °C, while the TRI-grafted sample began to degrade at a lower temperature range of 140 to 220 °C.
					Cyclic (TSA)		60 Cycles 400 ppm CO_2/N_2 25 °C 90 mL/min (120 min)	N_2 90 °C 90 mL/min (60 min)	• A 17% loss in uptake was observed within the first 20 cycles, with a final cyclic capacity of 0.32 mmol/g.

Reference	Adsorbent	Support material	Active Component	Loading (wt%)	Mode of Experiment		Thermal stability		Remarks
							Adsorption	Regeneration	
Choi et al. (2011)[62]	PEI/Silica	CARiACT G10 Silica	bPEI (Mw 800) (impregnation)	45	Cyclic (TSA)	G.A.	4 cycles		• 30% capacity decrease for PEI/Silica with final cyclic capacity of 1.65 mmol/g.
	A-PEI/silica		bPEI (Mw 800) (impregnation) and APTES as stabilizer				400 ppm CO_2/Ar (D) 25 °C 100 mL/min (24 h)	Ar 110 °C 100 mL/min (3 h)	• Minor decrease for A-PEI/silica and T-PEI/silica about 10 and 2%, respectively, showing positive effect of stabilizers on cyclic stability.
	T-PEI/silica		bPEI (Mw 800) (impregnation) and titanium (IV) propoxide ($C_{12}H_{28}O_4Ti$) as stabilizer		C.E.		Initial decomposition temperatures were observed using DSC thermograms.		• Better thermal stability in the presence of additives.
Choi et al. (2012)[63]	ED-Mg/DOBDC	Mg/DOBDC	ED (grafting)	5.5	C.E.	G.A.	4 cycles		• Stable cyclic stability of about 1.5 mmol/g was reported.
							400 ppm CO_2/Ar (D) 25 °C 100 mL/min (12 h)	Ar 120 °C 100 mL/min (3 h)	
Darunte et al. (2016)[19]	MIL-101(Cr)-PEI	MIL-101(Cr)	bPEI (Mw 800) (impregnation)	1.06 mmol/g	Cyclic (TSA)	G.A.	3 cycles		• Better cyclic stability for the TERN-grafted sample despite lower capture capacity.
	MIL-101(Cr)-TREN		TREN (impregnation)	2.67 mmol/g			400 ppm CO_2/He (D) 25 °C 90 mL/min (6 h)	He 110 °C 90 mL/min (3 h)	• Acceptable cyclic stability of MIL-101(Cr)-PEI with less than 5% capacity decrease after 3 cycles.
			TREN (grafting)	2.63 mmol/g					
Elfving et al. (2021) [64]	Proprietary aminoresin	Resin with matrix of polystyrene	Primary-amine groups	N.A.	Cyclic (TSA)	P.B.	19 cycles		• 7% adsorption capacity decrease from 0.57 to 0.53 mmol/g.
							400 ppm CO_2/N_2 (D) 25 °C 1000 mL/min	N_2 100 °C	
Gadipelli et al. (2015)[65]	5.0TEPA@MDCM	MOF-derived carbon monolith (MDCM)	TEPA (impregnation)	83	Cyclic (TSA)	G.A.	4 Cycles (50 min cycles)		• 6% capacity loss was recorded.
	6.0TEPA@MDCM			86			15% CO_2/N_2 (H) 75 °C 1 bar 50 mL/min	N_2 100 °C 50 mL/min	• sample encountered 17% capacity decrease.
	4.4TEPA@ActGO	Activated Graphene Oxide (ActGO)		81					• 36% uptake loss was reported.
	4.0TEPA@MDCM	MOF-derived carbon monolith (MDCM)		80			82 cycles		• About 30% CO_2 capture capacity decrease was observed.
							100% CO_2 (H) 75 °C 1 bar 50 mL/min (10 min)	N_2 100 °C 50 mL/min (20 min)	

Reference	Adsorbent	Support material	Active Component	Loading (wt%)	Mode of Experiment		Thermal stability		Remarks
							Adsorption	Regeneration	
Goeppert et al. (2019)[15]	TEPA/50S	Sipernat 50S silica	TEPA (impregnation)	50	Cyclic (CSA)	G.A.	50 cycles		• Steady weight drop over 50 cycles.
	TEPA-PO-1-2/50S		TEPA (impregnation) PO-Modified				95% CO_2/N_2 85 °C 60 mL/min (15 min)	N_2 85 °C 60 mL/min (5 min)	• Stable cyclic capacity for all epoxide-modified adsorbents: 2.16, 2.4, and 1.93 $mmol_{CO2}/g$ for TEPA-PO-1-2/50S, PEHA-PO-1-2/50S, PEHA-BO-1-2/50S, respectively. • 1% weight loss for TEPA-PO-1-2/50S over 50 cycles.
	PEHA-PO-1-2/50S		PEHA (impregnation) PO-Modified						
	PEHA-BO-1-2/50S		PEHA (impregnation) BO-Modified						
	TEPA/50S		TEPA (impregnation)		C.E.		Mass loss observed under N_2 at 70 and 100 °C for 20 h following by CO_2 adsorption measurement (under 95% CO_2 in N_2).		• ≈ 7.6 and 38% mass loss for TEPA/50S at 70 and 100 °C. • 62–78% capacity loss for TEPA/50S was at different adsorption temperatures. • LPEI and PEHA-loaded samples were more stable with about 1% and 7.6% weight loss (less than 10% capacity decrease).
	PEHA/50S		PEHA (impregnation)						
	LPEI25k/50S		lPEI (Mw 25000) (Impregnation)						
Guo et al. (2015)[66]	PTNT-60	Protonated titanate nanotube (PTNT)	TEPA (impregnation)	60	Cyclic (TSA)	P.B.	8 cycles		• Total capacity loss of 6% with final cyclic capacity of 3.87 mmol/g.
							10% CO_2/N_2 75 °C 10 mL/min	N_2 100 °C 20 mL/min (1 h)	
Guo et al. (2018)[67]	silica aerogel supported K_2CO_3	Silica aerogel	K_2CO_3 (impregnation)	20	Cyclic (TSA)	P.B.	10 cycles		• 5% capacity decrease in cyclic test with final uptake of 1.26 $mmol_{CO2}/g$. • The potassium carbonate utilization efficiency decreased from 88.62 to 83.74%.
							1% CO_2, 2% H_2O/N_2 (H) 20 °C 500 mL/min	N_2 200 °C 500 mL/min	
He et al. (2012)[68]	RFAS	Silica	APTES (grafting)	8.07 $mmol_N/g$	Cyclic (TSA)	P.B.	10 cycles		• A slight decrease in capacity was reported.
							1% CO_2/N_2 25 °C 300 mL/min	N_2 80 °C 300 mL/min	
Hosseini and Jahandar Lashaki (2023)[3]	PEI-600	CARiACT G-10 silica	bPEI (Mw 600) (impregnation)	40	Cyclic (TSA)	G.A.	50 cycles		• ≈ 1% capacity loss with final cyclic capacity of 1.51 and 1.38 mmol/g for PEI-600 and PEI-1800, respectively. • ≈ 55% amine and 29% capacity loss for attributed to evaporation of TEPA with final cyclic capacity of 1.55 mmol/g.
	PEI-1200		bPEI (Mw 1200) (impregnation)				400 ppm CO_2/N_2 (D) 25 °C 100 mL/min (120 min)	N_2 (D) 100 °C 100 mL/min (15 min)	
	PEI-1800		bPEI (Mw 1800) (impregnation)						
	TEPA		TEPA (impregnation)						

Reference	Adsorbent	Support material	Active Component	Loading (wt%)	Mode of Experiment		Thermal stability		Remarks
							Adsorption	Regeneration	
Hunt et al. (2024)[69]	Lewatit VPOC1065	Polystyrene-divinylbenzene	Primary amine	N.A.	Cyclic (TVSA)	G.A.	180 cycles 10 % CO_2/N_2 (D) 50 °C (15 min)	N_2 105 °C (10 min)	• 5.47% capacity loss recorded.
Irani et al. (2016)[70]	$TiO(OH)_2$/TEPA	$TiO(OH)_2$	TEPA (impregnation)	60	Cyclic (TSA)	P.B.	10 cycles 1 v% CO_2/N_2 (H) 60 °C 300 mL/min 1 v% H_2O (until C = C_0)	N_2 100 °C 300 mL/min	• The capacity decreased from 3.1 mmol/g to 2.5 mmol/g (19.3% decrease).
Irani et al. (2017)[71]	MCNTs/TEPA	Multi walled carbon nanotubes (CNTs)	TEPA (impregnation)	75	Cyclic (TSA)	P.B.	10 cycles 10 v% CO_2/ 1 v% H_2O/N_2 (H) 65 °C 300 mL/min (until C = C_0)	N_2 90 °C 300 mL/min	• 20% capacity loss across 10 cycles with final cyclic capacity of 4 mmol/g.
Jung et al. (2016)[40]	SG/TEPA-7N	Silica gel	TEPA (impregnation)	30.4	C.E.	G.A.	Pure CO_2 (D) 25–160 °C (30 min)		• Thermal stability was defined as SG/TEPA-7N > 3N-SG/TEPA-7N > 1N-SG/TEPA-7N. • Stronger interaction between impregnated TEPA and longer hydrocarbon chains of aminosilanes.
	1N-SG/TEPA-7N		TEPA (impregnation) + APTMS (grafting)	23.3					
	3N-SG/TEPA-7N		TEPA (impregnation) + TRI (grafting)	13.8					
Keller et al. (2018)[72]	PEI-CNT-microtubes	Multi-walled carbon nanotube based (MWCNT) microtubes	bPEI (Mw 800) (impregnation)	20	Cyclic (TSA)	G.A.	10 cycles 0.15 v% CO_2/N_2 30 °C 150 mL/min (10 min)	N_2 90 °C 150 mL/min (20 min)	• 10% capacity decrease. • 1% mass loss of microtube.
Kong et al. (2016)[73]	AHSA	Polysilsesquioxane	APTES	7.64 mmol/g	Cyclic (TSA)	P.B.	30 cycles 1% CO_2/N_2 (D,H) 50 °C 300 mL/min 1% moisture (until C ≈ C_0)	N_2 80 °C 300 mL/min (until C ≈ 0)	• About 3% capacity decrease under humid conditions. • Stable uptake capacity under dry conditions.

Reference	Adsorbent	Support material	Active Component	Loading (wt%)	Mode of Experiment		Thermal stability		Remarks
							Adsorption	Regeneration	
Kong et al. (2016)[74]	AHTSA	Polysilsesquioxane	APTES	8.47 mmol/g	Cyclic (TSA)	P.B.	15 cycles 0.04%, 1% and 10% CO_2/N_2 (D) 30 °C 300 mL/min	N_2 90 °C 300 mL/min	• No significant capacity decline was recorded.
Kulkarni et al. (2023)[75]	HS-TEPA-70	Hierarchical silica particles	TEPA (impregnation)	70	Cyclic (TSA)	G.A.	10 cycles 400 ppm CO_2/He (D) 30 °C (4.2 h)	N_2 110 °C 20 mL/min (30 min)	• 22% capacity loss over 10 cycles with 150 mg/g cyclic capture capacity.
	pelletized HS-TEPA-70						5 cycles 400 ppm CO_2/He (D) 30 °C (12 h)	N_2 110 °C 20 mL/min (30 min)	• Stable CO_2 capacity over 5 cycles.
Kumar et al. (2020)[20]	Ph-3- ED/SBA-15	SBA-15	Aromatic core with ethylenediamine (ED) (impregnation)	50 and 60	Cyclic (TSA)	G.A.	25 cycles 400 ppm CO_2/He (D) 35 °C (1 h)	He 90 °C (10 min)	• Stable cyclic stability for all samples. • Slight capacity increase for sample with 60 wt% loading.
	Ph-3-PD/SBA-15		Aromatic core with propylenediamine (PD) (impregnation)						
Kumar et al. (2022)[12]	PEI50/SBA-15	SBA-15	bPEI (Mw 600) (impregnation)	50	Cyclic (TSA)	P.B.	10 cycles 400 ppm CO_2/He (H) 25 °C RH=60% atmospheric pressure 100 mL/min (4 h)	He (H) 80 °C 30 mL/min (30 min)	• TETA had capacity loss after each cycle with a total capacity decrease of 30%.
	TEPA50/SBA-15		TEPA (impregnation)						
	TETA50/SBA-15		TETA (impregnation)						
Kuwahara et al. (2012)[76]	PEI/SBA-15	SBA-15	bPEI (Mw 800) (impregnation)	30	Cyclic (TSA)	G.A.	4 cycles 400 ppm CO_2/Ar (D) 25 °C 100 mL/min (12 h)	Ar 110 °C 100 mL/min (3 h)	• Incorporating Zr into silica support improved cyclic stability as well as capture capacity and amine efficiency.
	PEI/Zr7-SBA-15	Zr-SBA-15		7 mol% Zr/30 wt% PEI					

Reference	Adsorbent	Support material	Active Component	Loading (wt%)	Mode of Experiment		Thermal stability		Remarks
							Adsorption	Regeneration	
Kuwahara et al. (2012)[77]	PEI/SBA-15	SBA-15	bPEI (Mw 800) (impregnation)	30	Cyclic (TSA)	G.A.	4 cycles 400 ppm CO_2/Ar (D) 25 °C 100 mL/min (12 h)	Ar 110 °C 100 mL/min (3 h)	• Incorporating Zr into silica support improved cyclic stability as well as capture capacity and amine efficiency.
	PEI/$Zr_{7.0}$-SBA-15	Zr-SBA-15							
	PEI/$Ti_{4.3}$-SBA-15	Ti-SBA-15							
Kwon et al. (2019)[78]	S_H-PEI_LV	Hierarchical meso-/macroporous silica (H-SiO_2)	bPEI (Mw 800) (impregnation)	67.1	Cyclic (TSA)	P.B.	5 cycles 400 ppm CO_2/He (D,H) 30 °C RH = 19% 100 mL/min	He 110 °C 100 mL/min (6 h)	• Stable cyclic performance under dry conditions. • 15% capacity decrease after 5 cycles under humid conditions.
Lawson et al. (2019)[79]	PEI-MIL-101P	MIL-101 (MOF)	bPEI (Mw 800) powder (impregnation)	5.5 $mmol_N/g$	Cyclic (TSA)	G.A.	5 cycles 3000 ppm CO_2/N_2 (D) 25 °C 60 mL/min (180 min)	N_2 120 °C 40 mL/min (60 min)	• bPEI-impregnated sample had the highest capture capacity with final uptake of 2.1 mmol/g.
	PEI-MIL- $101M_B$		bPEI Monolith (pre-impregnation)	5.3 $mmol_N/g$					• Pre-impregnated adsorbent had higher CO_2 adsorption capacity. • Stable cyclic capacity of 1.7 mmol/g.
	PEI-MIL-$101M_A$		bPEI Monolith (post-impregnation)	3.2 $mmol_N/g$					• Constant cyclic capacity of 1.4 mmol/g.
	TEPA-MIL-101P		TEPA powder (impregnation)	4 $mmol_N/g$			5 cycles 3000 ppm CO_2/N_2 (D) 25 °C 60 mL/min (180 min)	N_2 120 °C 40 mL/min (10 min)	• About 20% capacity loss for the powder adsorbent with final cyclic capacity of approximately 1.35 mmol/g.
	TEPA-MIL- $101M_B$		TEPA Monolith (pre-impregnation)	3.5 $mmol_N/g$					• Enhanced cyclic stability due to grafting occurred during disinfection step.
	TEPA-MIL-$101M_A$		TEPA Monolith (post-impregnation)	0.8 $mmol_N/g$					• 20% capacity decrease with lowest cyclic capacity of 0.3 mmol/g was reported.
Liu et al. (2012)[80]	MSF-T-1.0	Mesocellular silica foam (MCF)	TEPA (impregnation)	TEPA / support = 1	Cyclic (CSA)	G.A.	10 cycles 15% CO_2 (D) 75 °C 50 mL/min (40 min)	N_2 75 °C 50 mL/min (80 min)	• Significant capacity loss for impregnated sample. • Enhanced cyclic stability due to strong chemical bonds created during grafting process.
	MSF-CT-1.0		TEPA (grafting)				50 cycles 15% CO_2 (D) 75 °C 50 mL/min (40 min)	N_2 75 °C 50 mL/min (80 min)	• CO_2 capture capacity decreased after over 50 cycles caused by urea formation.

Reference	Adsorbent	Support material	Active Component	Loading (wt%)	Mode of Experiment		Thermal stability		Remarks
							Adsorption	Regeneration	
Liu et al. (2015)[16]	DETA-MCM41	MCM-41 mesoporous silica	DETA (impregnation)	40	C.E.	G.A.	TGA mass loss was observed up to 700 °C in N_2.		• The mass losses of samples were in the following order: EDA-MCM41 < DETA-MCM41 < TEPA-MCM41 < PEHA-MCM41 • The initial decomposition temperature was higher for amines with higher chain length.
	EDA-MCM41		EDA (impregnation)						
	PEHA-MCM41		PEHA (impregnation)						
	TEPA-MCM41		TEPA (impregnation)						
Liu et al. (2020)[81]	EtSNTs-50	Ethane-silica nanotubes	bPEI (MW 600) (impregnation)	50	Cyclic (TSA)	P.B.	8 cycles		• No change observed in breakthrough time after 8 cycles.
							400 ppm CO_2/N_2 30 °C 60 mL/min (until equilibrium)	N_2 100 °C 45 mL/min (2 h)	
Miao et al. (2021)[82]	PEI/SBA-15	SBA-15	bPEI (Mw 800) (impregnation)	25–75	Cyclic (TSA)	G.A.	10 cycles		• Stable uptake capacity after 10 cycles. • Minor weight loss at the end of the cyclic experiment.
	TEPA/SBA-15		TEPA (impregnation)				400 ppm CO_2/N_2 (D) 25 °C 100 mL/min (60 min)	N_2 110 °C 100 mL/min (15 min)	
					C.E.		100% N_2 in the range of 50 to 900 °C		• Better stability of PEI/SBA-15 than TEPA/SBA-15.
Min et al. (2022)[83]	PEI-ePTFE/silica	Expanded poly(tetrafluoroethylene) (ePTFE)/mesoporous silica	bPEI (Mw 800) (impregnation)	≈ 34	Cyclic (TSA)	G.A.	10 Cycles		• 6% pseudo-equilibrium capacity decrease was reported.
							400 ppm CO_2/He (D) 35 °C 90 mL/min (3 h)	He 110 °C 90 mL/min (30 min)	
						P.B.	10 Cycles		• The capture capacity was increased in the presence of moisture. • Stable performance over humid cycles.
							400 ppm CO_2/N_2 (H) 35 °C RH = 50% 100 mL/min (6 h)	N_2 90 °C 100 mL/min (2 h)	
	Structured PEI-ePTFE/silica laminate sheets			≈ 38	Cyclic (S-TSA)	Adsorption apparatus	5 Cycles		• Stable capture capacity over tested cycles.
							400 ppm CO_2/N_2 (D) 35 °C 550 mL/min	S-TSA + N_2 as sweeping gas	
Pang et al. (2018)[5]	PPI/SBA-15	SBA-15	lPPI (Mw 1000) (impregnation)	50	C.E.	G.A.	50 cycles		• No performance decline was observed.
							Ultra-zero grade air (D) 35 °C	N_2 110 °C	

Reference	Adsorbent	Support material	Active Component	Loading (wt%)	Mode of Experiment		Thermal stability		Remarks
							Adsorption	Regeneration	
Park et al. (2020)[7]	PPG/SBA-15	SBA-15	PPG (impregnation)	50	Cyclic (TSA)	G.A.	5 cycles		• Lower thermal cyclic stability of PPG-based adsorbent than PEI-based one.
					C.E.		10% CO_2/N_2 30 °C (6 h)	He 120/110 °C (1 h)	• PPG/SBA-15 showed lower pseudo-equilibrium capacity than PEI/SBA-15 but reached faster under DAC conditions.
	PEI/SBA-15		bPEI (impregnation)	37			He 100/120 °C (6 h)		• Lower capacity decrease at regeneration temperature of 100 °C than 120 °C.
Parvazinia et al. (2018)[84]	Lewatit VPOC1065	Polystyrene-divinylbenzene	Primary amine	N.A.	Cyclic (TSA)	G.A.	275 cycles		• 4.84% capacity loss with final cyclic uptake of about 0.67 mmol/g.
							10% CO_2/N_2 (D) 50 °C 50 mL/ min (20 min)	N_2 105 °C 50 mL/ min (10 min)	
	Purolite A109						40 cycles		• 11.24% capacity loss over 40 cycles with final cyclic uptake of approximately 0.23 mmol/g.
							10% CO_2/N_2 (D) 50 °C 50 mL/ min (20 min)	N_2 90 and 105 °C 50 mL/ min (10 min)	
Priyadarshini et al. (2023)[85]	PEI-impregnated γ-Al_2O_3	γ-Al_2O_3	bPEI (Mw 800) (impregnation)	20	Cyclic (TSA)	G.A.	5 cycles		• Stable cyclic uptake capacity under both ambient and sub-ambient conditions, with final capacity of about 0.5 and 0.71 mmol/g, respectively.
							400 ppm CO_2/He (D) 25 °C 90 mL/min (2 h)	He 50 °C 90 mL/min (2 h)	
							10 cycles		
							400 ppm CO_2/He (D) –20 °C 90 mL/min (2 h)	He 50 °C 90 mL/min (2 h)	
				40			5 cycles		• Stable cyclic uptake capacity under both ambient and sub-ambient conditions, with final capacity of about 1.05 and 0.65 mmol/g, respectively.
							400 ppm CO_2/He (D) 25 °C 90 mL/min (2 h)	He 60 °C 90 mL/min (2 h)	
							10 cycles		
							400 ppm CO_2/He (D) –20 °C 90 mL/min (2 h)	He 60 °C 90 mL/min (2 h)	

Reference	Adsorbent	Support material	Active Component	Loading (wt%)	Mode of Experiment		Thermal stability		Remarks
							Adsorption	Regeneration	
continued Priyadarshini et al. (2023)[85]	TEPA-impregnated γ-Al_2O_3		TEPA (impregnation)	20			5 cycles		• Stable cyclic uptake capacity under both ambient and sub-ambient conditions, with final capacity of about 0.9 and 1.1 mmol/g, respectively.
							400 ppm CO_2/He (D) 25 °C 90 mL/min (2 h)	He 60 °C 90 mL/min (2 h)	
							10 cycles		
							400 ppm CO_2/He (D) –20 °C 90 mL/min (2 h)	He 60 °C 90 mL/min (2 h)	
				40			5 cycles		• Stable cyclic uptake capacity under both ambient and sub-ambient conditions, with final capacity of about 1.35 and 0.9 mmol/g, respectively.
							400 ppm CO_2/He (D) 25 °C 90 mL/min (2 h)	He 70 °C 90 mL/min (2 h)	
							10 cycles		
							400 ppm CO_2/He (D) –20 °C 90 mL/min (2 h)	He 70 °C 90 mL/min (2 h)	
Qi et al. (2011)[86]	MC400/10PEI%83	Mesoporous silica capsules	bPEI (Mn 423) (impregnation)	83	Cyclic (TSA)	P.B.	50 cycles		• Better cyclic stability of PEI-loaded adsorbent compared to TEPA due to higher PEI boiling point.
	MC400/10TEPA%83		TEPA (impregnation)				Pure CO_2 (D) 75 °C (10 min)	N_2 100 °C 25 mL/min (10 min) or N_2 75 °C 25 mL/min (25 min)	
Rao et al. (2018)[87]	50% PEI−MCM-41	MCM-41	bPEI (Mn 600) (impregnation)	50	Cyclic (TVSA)	P.B.	5 cycles		• PEI-impregnated sample faced 12.65% and 14.22% uptake loss after the first cycle and the 5th cycle with final capacity of 3 mmol/g. • 5.19% capacity decrease was reported for APTES grafted sample with final CO_2 uptake of about 2.3 mmol/g.
	50% APTS−MCM-41		APTES (grafting)				Pure CO_2 25 °C 1 bar 50 mL/min	100 °C Vacuum pressure (1 h)	
					C.E.	G.A.	Weight loss was observed up to 600 °C.		• PEI degradation started at 100 °C and APTES decomposition initiated at 150 °C.

Reference	Adsorbent	Support material	Active Component	Loading (wt%)	Mode of Experiment		Thermal stability		Remarks
							Adsorption	Regeneration	
Rim et al. (2022)[88]	MIL-101(Cr)_50 wt% PEI	MIL-101(Cr)	bPEI (Mw 800) (impregnation)	50	Cyclic (TSA)	G.A.	15 cycles		• Stable CO_2 adsorption capacity over 15 cycles for both amine-impregnated samples.
	MIL-101(Cr)_30 wt% TEPA		TEPA (impregnation)	30			400 ppm CO_2/He (D) 25 and -20 °C 90 mL/min (2 h)	He 25 and 60 °C 90 mL/min (2 h)	
						P.B.	5 cycles		
							400 ppm CO_2/He (H) –20 °C 50 mL/min (2 h)	N_2 25 °C 90 mL/min (2 h)	
Rodríguez-Mosqueda et al. (2019)[89]	K-2	Activated carbon honeycombs	K_2CO_3 (impregnation)	5	Cyclic (TSA)	P.B.	10 cycles		• K_2CO_3- and Na_2CO_3-impregnated samples showed stable cyclic performance. • K-based adsorbents had higher CO_2 capture capacity than Na-based samples.
	Na-AC		Na_2CO_3 (impregnation)				Air (H) 30 °C RH = 26% 5000 mL/min ($C = C_0$)	N_2 210 °C 5000 mL/min (1 h)	
Sandhu et al. (2016)[90]	Si/PEI-40	CARiACT G-10 silica	bPEI (Mw 800) (impregnation)	40	G.A.		100% N_2 in the range of 50 to 650 °C		• PEI was stable below 150 °C.
Sanz-Pérez et al. (2018)[91]	HMS-10a-PEI (50)	HMS mesoporous silica	bPEI (Mw 800) (impregnation)	50	Cyclic (TSA)	G.A.	4 cycles		• Stable capture capacity over 4 cycles for both samples.
	HMS-12a-PEI (50)						Pure CO_2 45 °C 1 bar 100 mL/min (3 h)	N_2 110 °C 100 mL/min (2 h)	
Sayari and Belmabkhout (2010)[41]	PEI-PE-MCM-41	PE-MCM-41 (silica support)	bPEI (impregnation)	50	Cyclic (TSA)	G.A.	22–700 cycles		• Better cyclic stability under humid conditions due to prevention in urea formation. • 14% capacity decrease after 40 cycles T_{ads} = 50 °C and T_{reg} = 120 °C for the TRI sample.
	MONO-PE-MCM-41		APTMS (grafting)	4.3 mmol/g			Pure CO_2 (D,H) 50–105 °C atmospheric pressure RH=74% (25 °C)–0.4% (150 °C) 50 mL/min (30 min)	N_2 (D,H) 70–120 °C atmospheric pressure 50 mL/min (30 min)	
	TRI-PE-MCM-41		TRI (grafting)	7.9 mmol/g					

Reference	Adsorbent	Support material	Active Component	Loading (wt%)	Mode of Experiment		Thermal stability		Remarks
							Adsorption	Regeneration	
Sayari et al. (2012)[8]	pMono	SBA-15	APTMS (grafting)	28	Cyclic (TSA)	G.A.	30 cycles		• 66% uptake loss was reported.
	sMono-1		TMMAPS (grafting)	26			Pure CO_2 (D) 50 °C 1 bar (30 min)	Pure CO_2 (D) 130 °C 1 bar (30 min)	• Samples loaded with components containing only secondary amines were stable over tested cycles with less than 1% capacity loss.
	sMono-2		N-butylaminopropyl trimethoxysilane (grafting)	29					
	DI		DI (grafting)	24					• 72% capacity decrease was recorded for diamine and TRI containing samples.
	TRI		TRI (grafting)	37					
	BPEI		bPEI (Mn 600) (impregnation)	50					• Adsorbent experienced 76% uptake decrease.
	LPEI		lPEI (Mw 2500) (impregnation)	40			30 cycles		• Sample had 50% capacity decline.
							100% CO_2 (D) 50 °C 1 bar (30 min)	100% CO_2 150 °C 1 bar (30 min)	
	PALL		PAA (Mw 17000) (impregnation)	40			30 cycles		• 62% uptake loss was reported.
							100% CO_2 (D) 100 °C 1 bar (30 min)	100% CO_2 160 °C 1 bar (30 min)	
Sayari et al. (2012)[42]	pMono	Pore-expanded MCM-41 (PE-MCM-41)	APTMS (grafting)	4.6 mmol/g	Cyclic (TSA)	G.A.	60 cycles		• Secondary amine had stable cyclic capacity, while primary amine lost 21% of its initial uptake capacity. • Capacity loss was linked to urea formation according to NMR and DRIFT results.
	sMono		MAPS (grafting)	3.67 mmol/g			100% CO_2 (D) 55 °C 1 bar 50 mL/min (30 min)	N_2 120 °C 50 mL/min (30 min)	
Sayari et al. (2016)[92]	PME/PEI(40)	Pore-expanded MCM-41 (PE-MCM-41)	bPEI (Mw 800) (impregnation)	40	Cyclic (TSA)	P.B.	20 cycles		• 4.6% and 2% capacity decrease in dry and humid conditions, respectively.
							400 ppm CO_2/N_2 (D,H) RH = 64% 25 °C (until saturation)	N_2 90 °C 40 mL/min (1 h)	

Reference	Adsorbent	Support material	Active Component	Loading (wt%)	Mode of Experiment		Thermal stability		Remarks
							Adsorption	Regeneration	
Sehaqui et al. (2015)[93]	NFC/ PEI-19	Oxidized nanofibrillated cellulose (NFC)	bPEI (impregnation)	19	Cyclic (TSA)	P.B.	5 cycles		• Stable performance for samples below 44 wt% PEI.
	NFC/ PEI-31			31			Air (H) 25 °C RH= 80% 1000 mL/min	Dry N_2 (H) 85 °C RH= 40% 500 mL/mi	
	NFC/ PEI-44			44					
	NFC/ PEI-52			52					
	NFC/ PEI-62			62					
					C.E.	G.A.	In the range of 100 – 600 °C		• The degradation temperature was increased by increasing the PEI content of the sample.
Spinu et al. (2024)[94]	PEHA-40	Silica gel	PEHA (Mw 232.37) (impregnation)	40	Cyclic (TSA)	G.A.	26 cycles		• bPEI-loaded samples exhibited greater thermal stability compared to PEHA-impregnated adsorbents. • Samples with a higher amine loading retained their capture capacity more effectively than those with a lower loading. • High-Mw bPEI had superior thermal stability.
	PEHA-50			50			5% CO_2/N_2 75 °C (12 min)	N_2 100 °C (12 min)	
	PEI8-40		bPEI (Mw 800) (impregnation)	40					
	PEI8-50			50					
	PEI12-40		bPEI (Mw 1200) (impregnation)	40					
Sujan et al. (2019)[11]	PGA/SBA-15	SBA-15	PGA (impregnation)	45 and 55	Cyclic (TSA)	G.A.	20 cycles		• Capacity loss for the samples impregnated with high molecular weight PGA.
							10% CO_2/N_2 35 °C (1 h)	He 90 °C (20 min)	
Sujan et al. (2019)[95]	PEI-CA-SiO_2 fibers	Polymer/silica fiber	bPEI (Mw 800) (impregnation)	0.7 g_{PEI}/g_{SiO2}	Cyclic (TSA)	P.B.	20 cycles (D)		• 16% and slight breakthrough capacity reduction under dry and wet conditions, respectively. • About 2% mass loss at TGA with no CO_2 capacity decrease.
							380 ppm CO_2/397 ppm He/ N_2 (D) 35 °C 100 mL/min (4 to 5 h)	N_2 (D) 90 °C 20 mL/min (25 min)	
							6 cycles (H)		
							380 ppm CO_2/397 ppm of He/balance N_2 mixture 35 °C RH=85% 200 mL/min (4 to 5 h)	380 ppm CO_2/397 ppm of He/balance N_2 mixture 35 °C RH=85% 200 sccm (4 to 5 h)	
						G.A.	10 cycles		
							395 ppm CO_2/He 35 °C (3h)	395 ppm CO_2/He 35 °C (3h)	

Reference	Adsorbent	Support material	Active Component	Loading (wt%)	Mode of Experiment		Thermal stability		Remarks
							Adsorption	Regeneration	
Thakkar et al. (2007)[96]	TEPA-ZY	Kaolin-based zeolite Y	TEPA (impregnation)	10	Cyclic (TSA)	G.A.	5 cycles 5000 ppm CO_2/N_2 (D) 25 °C	N_2 100 °C (1 h)	• Stable capture capacity over 5 cycles.
Veselovskaya et al. (2021)[97]	ZK-3	Mesoporous zirconia aerogel	K_2CO_3 (impregnation)	23	Cyclic (TSA)	P.B.	14 cycles 390–450 ppm CO_2 (H) 25 °C RH=25% 2300 mL/min (6 h)	Ar 200 °C 500 mL/min (1 h)	• Stable cyclic performance with capture capacity of 4.6–4.7 wt % of adsorbent.
Wang et al. (2012)[98]	50 wt% PEI/SBA-15	SBA-15	bPEI (Mn 423) (impregnation)	50	Cyclic (TSA)	TPD	20 cycles 400 ppm CO_2/N_2 75 °C (30 min)	He 110 °C (20 min)	• Stable capture capacity over 20 cycles.
Wang et al. (2013)[99]	PEI-15/SBA-15	SBA-15	bPEI (Mw 423) (impregnation)	15–70	C.E.	G.A.	TGA mass loss was observed up to 600 °C.		• By increasing PEI loading up to 60 wt%, the decomposition peak temperature was decreasing, whereas above 60 wt% the temperature started to increase.
Wang et al. (2015)[100]	MC-55-5	Mesoporous carbon	bPEI (Mw 600) (impregnation)	55 wt% of PEI + 5 wt% of Span 80	Cyclic (TSA)	P.B.	10 cycles 5000 and 400 ppm CO_2/N_2 25 °C 50 mL/min	N_2 110 °C 50 mL/min	• Stable capture capacity over 10 cycles with only 2% and 3% drop in adsorption capacity at CO_2 concentrations of 5000 and 400 ppm, respectively,
Xu et al. (2020)[101]	PEI "snow"	-	bPEI (30 wt% solution, Mn 2500) (cross-linking)	N.A.	Cyclic (TSA)	P.B.	10 cycles Lab air 2000 mL/min (C=C$_0$)	Water steam 120 °C (30 min)	• Stable performance over 10 cycles.
					C.E.	G.A.	Assessed in TA between room temperature and 300 °C.		• 26.4% residual mass at 300 °C, similar to initial dry PEI.
Yoo et al. (2020)[34]	APS	Silica	APTMS (grafting)	0.92–1.28 $mmol_{Si}/g$	Cyclic (TSA)	G.A.	4 cycles 400 ppm CO_2/He 25 °C (3 h)	He 110 °C (3 h)	• Normalized CO_2 uptake decreased by about 5%.
	L-ethyl		DI (grafting)						
	L-propyl		L-propyl (grafting)						
	B-ethyl		B-ethyl (grafting)						
	B-propyl		B-propyl (grafting)						

Reference	Adsorbent	Support material	Active Component	Loading (wt%)	Mode of Experiment		Thermal stability		Remarks
							Adsorption	Regeneration	
Yu et al. (2017)[102]	Lewatit	Ion-exchange resin	aminomethylene (Commercial Adsorbent)	N.A.	C.E.	P.B.	0.8 atm CO_2/N_2 120 °C (72h)		• Degradation increased by T and P_{CO2} increase, 9% capacity decrease at 120 °C for 80% CO_2 case.
							1 atm of CO_2 150 °C (170 h)		
							100% N_2 100, 150, 200 °C (50 h)		• Thermally stable until 150 °C, degradation (uptake decrease = 39%) with temperature increase to 200 °C.
Zhang et al. (2015)[103]	FS-LPEI(5000)-47.8	Aerosil® 380 hydrophilic fumed silica	lPEIs (Mn 5000) (impregnation)	47.8	C.E.	G.A.	N_2 (D) 70 and 100 °C (20 h)		• Minor capacity decrease, 5.6% due to amine group leaching.
	FS-LPEI(25000)-44.5	Aerosil® 380 hydrophilic fumed silica	lPEI (Mn 25000) (impregnation)	44.5	Cyclic (CSA)		35–200 cycles 95% CO_2/N_2 or 10% CO_2/N_2 (D,H) Saturated with water vapor at 25 °C 55 or 75 °C (10 min)	N_2 adsorption and desorption conducted isothermally 55 or 75 °C (15 min)	• Stable cyclic capacity both under dry and humid conditions. • After 100 cycles under 95% dry CO_2 at 75 °C and 180 cycles at 55 °C the adsorbent exhibited stable capture capacity, 135 mg_{CO2}/g, and 115 mg_{CO2}/g, respectively. • Under 10% CO_2 stream at 55 °C the stable capacity of 120 mg_{CO2}/g was reached over 35 cycles.
	FS-LPEI(2500)		lPEI (Mn 2500) (impregnation)	45.5			10 cycles 95% CO_2/N_2 85 °C (10 min)	N_2 85 °C (15 min)	• Stable capacity over 10 cycles for samples with LPEI having different Mws.
	FS-LPEI(5000)		lPEI (Mn 5000) (impregnation)	47.8					
	FS-LPEI(10000)		lPEI (Mn 10000) (impregnation)	48.7					
	FS-LPEI(25000)		lPEI (Mn 25000) (impregnation)	44.5					
Zhang et al. (2018)[104]	SBA-15(p)-60TEPA (SP60T)	SBA-15(p) (uncalcined SBA-15)	TEPA (impregnation)	60	C.E	G.A.	9 cycles 20 v% CO_2/80 v% N_2 60 mL/min (1 h)	105 °C Vacuum pressure (1 h)	• 7.8% capacity decrease over 9 cycles with around 5.0 mmol/g cyclic capture capacity. • Improved cyclic stability due to formation of weak hydrogen-bond interaction between TEPA and P123 and silicon hydroxyl groups on the support surface.
	SBA-15-60TEPA	SBA-15							• 12% capacity loss over 9 cycles with around 4.45 mmol/g cyclic capture capacity. • TGA mass loss was also observed up to 600 °C. The initial decomposition temperature increased from 145 °C for TEPA impregnated onto uncalcined SBA-15.

Reference	Adsorbent	Support material	Active Component	Loading (wt%)	Mode of Experiment		Thermal stability		Remarks
							Adsorption	Regeneration	
Zhang et al. (2019)[105]	SBA-15(p)-AP-xT	SBA-15(p) (uncalcined SBA-15)	APTES (grafting) + TEPA (impregnation)	0–70	C.E.	G.A.	TGA mass loss was observed up to 600 °C.		• Grafting APTES had a positive effect on enhancing the thermal stability of TEPA-loaded adsorbent.
Zhang et al. (2022)[106]	TEPA@PAN-PMMA	Polyacrylonitrile(PAN)-poly(methyl methacrylate)(PMMA) porous hollow fibers	TEPA (grafting)	74.85% grafting degree	Cyclic (TSA)	P.B.	6 cycles		• 8% capacity loss with final cyclic uptake of 1.38 mmol/g.
							0.3% CO_2/N_2 (D) 25 °C 400 mL/min	N_2 80 °C 400 mL/min (60 min)	
				58.2% grafting degree	C.E.	G.A.	Weight loss was observed from 50 °C to 800 °C under N_2 with flow rate of 50 mL/min		• Weight loss between 150 °C and 280 °C was associated with the degradation of grafted TEPA.
Zhao et al. (2019)[107]	PEI-silica	Silica	PEI (MW 10000) (impregnation)	≈ 20	Cyclic (TSA)	G.A.	10 cycles		• No capacity decrease after 10 cycles under both dry and humid conditions.
							0.5% CO_2 (D,H) RT RH=90% (until C=0.1%)	N_2 90 °C RH=30% (18/20 min)	
					C.E.		Assessed in the range of 30 to 800 °C.		• Observed mass loss between 240 and 550 °C was attributed to PEI decomposition.
Zhao et al. (2022)[108]	$Mg_{0.55}Al$-O-TEPA67%	$Mg_{0.55}Al$-O	TEPA (impregnation)	67	Cyclic (TSA)	G.A.	80 cycles		• 9.4% and 9.6% capacity loss over 20 and 80 cycles with final uptake of 2.5 and 1.19 mmol/g, respectively.
							400 ppm CO_2/N_2 (D) 25 °C 40 mL/min (180 min)	N_2 100 °C 40 mL/min (15 min)	
							20 cycles		
	TEPA/SBA-15	SBA-15					400 ppm CO_2/N_2 (D) 25 °C 40 mL/min (100 min)	N_2 100 °C 40 mL/min (15 min)	• 19.9% capacity decrease with final uptake of about 1.5 mmol/g.
	TEPA/L-MgO	L-MgO		33					• 56.7% capacity lost with final cyclic capacity of approximately 0.25 mmol/g.
	TEPA/γ-Al_2O_3	γ-Al_2O_3		50					• 37% capacity decline with final value of about 1.5 mmol/g.

Table S2. Summary of studies on the **oxidative stability** of solid DAC adsorbents, including adsorbent types, experimental conditions, and key findings.

Reference	Adsorbent	Support material	Active Component	Loading (wt%)	Mode of Experiment		Oxidative stability		Remarks
							Adsorption	Regeneration	
Ahmadalinezhad et al. (2013)[36]	sMono	Pore-expanded mesoporous MCM-41 silica	TMMAPS (grafting)	3.51 $mmol_N/g$	C.E.		Oxidative treatment under pure air at 100 to 160 °C for 24 h following by CO_2 capacity measurement in a TGA device under pure CO_2 for 60 h.		• In the surface species formed by oxidative degradation of amine-grafted silica, imine, amide, and carboxyl functional groups were identified.
	TRI		TRI (grafting)	8.04 $mmol_N/g$					
Ahmadalinezhad and Sayari (2014)[109]	LPEI	SBA-15	lPEI (Mw 2500) (impregnation)	29.7	C.E.		Oxidative treatment under pure air at 80 to 120 °C for 24 h following by CO_2 capacity measurement in a TGA device under pure CO_2 at 75 °C for 60 h.		• lPEI-loaded sample had better stability than bPEI-based adsorbent, showing 54% capacity loss after treatment at 110 °C in comparison to 98% uptake decrease after oxidative treatment at 120 °C.
	BPEI		bPEI (Mn 600) (impregnation)	41.7					
Anyanwu et al. (2020)[54]	W-AG-150A	Silica gel	TRI (grafting)	5.2 mmolN/g	Mass loss observed in TGA		Under air flow until 800 °C		• Amine group oxidation occurred above 150 °C.
Bali et al. (2013)[10]	ALPEI	γ-Alumina	bPEI (Mw 800) (impregnation)	41.6	C.E.	P.B.	Treating samples under 21% or 5% O_2 in N_2 at 70 or 110 °C with flow rate of 15 mL/min for 20 h. The capture capacity was later measured in TGA using 10% CO_2 at 50 °C for 6 h.		• Higher oxidative degradation was reported for PEI sample as treatment temperature and O_2 concentration were increased. • PAA loaded sample exhibited great oxidative stability than PEI-impregnated samples is the same conditions.
	ALPAA		PAA (impregnation)	45.8					
Bollini et al. (2011)[33]	MCF_APS	Mesocellular Silica Foam (MCF)	APTMS (grafting)	2.39 $mmol_N/g$	C.E.		Accelerated oxidative treatment under O_2 stream at 25, 45, 75, 105, and 135 °C with flow rate of 20 mL/min for 24 h following by characterization and CO_2 capacity measurement in a TGA device with adsorption under 10% CO_2 at 45 °C for 30 min and regeneration under argon at 110 °C for 2 h.		• No capacity loss was reported for APS and DMAPS grafted adsorbents.
	MCF_DMAPS		DMAPS (grafting)	2.49 $mmol_N/g$					
	MCF_MAPS		MAPS (grafting)	2.28 $mmol_N/g$					• 20% and 90% CO_2 uptake decrease after treatment at 105 and 135 °C, respectively.
	MCF_DA		DI (grafting)	3.52 $mmol_N/g$					• 30% and 95% capacity decline after oxidative treatment at 105 and 135 °C, respectively.
Calleja et al. (2011)[32]	SBA-15-AP (N)-6	SBA-15	APTMS (grafting)	3.7 wt% Nitrogen	C.E.		Drying the synthesized adsorbents under ambient air at room temperature (20 °C) for 24 h and at 110 °C for 6, 24 and 72 h.		• 8% capacity loss was recorded at 110 °C for 72 h compared to dried sample at RT, with final capacity of 1.02 mmol/g.
	SBA-15-ED (NN)-6		DI (grafting)	5.7 wt% Nitrogen					• 68% capacity loss was observed at 110 °C for 72 h compared to dried sample at RT, with final capacity of 0.44 mmol/g.
	SBA-15-DT (NNN)-6		TRI (grafting)	7.3 wt% Nitrogen					• 80% capacity loss was reported at 110 °C for 72 h compared to dried sample at RT, with final capacity of 0.35 mmol/g.

Reference	Adsorbent	Support material	Active Component	Loading (wt%)	Mode of Experiment		Oxidative stability		Remarks
							Adsorption	Regeneration	
Didas et al. (2014)[45]	SBA-Ethyl-low	SBA-15	2-aminoethyltrimethoxysilane (grafting)	0.85 $mmol_N/g$	C.E.	P.B.	Subjected to pure O_2 gas at 135 °C for 20 h followed by CO_2 capture capacity measurement with 10% CO_2 in He for 3 h.		• All tested adsorbents were oxidatively stable.
	SBA-Ethyl			1.80 $mmol_N/g$					
	SBA-Propyl-low		APTMS (grafting)	0.74 $mmol_N/g$					
	SBA-Propyl			1.43 $mmol_N/g$					
Gebald et al. (2011)[110]	AEAPDMS-NFC-FD	Nanofibrillated cellulose (NFC)	AEAPDMS (grafting)	4.9 $mmol_N/g$	Cyclic (TSA)	P.B.	20 cycles		• Almost stable uptake capacity under humid conditions.
							Airflow 25 °C RH=40% 1000 mL/min (2 h)	Ar 90 °C 800 mL/min (1 h)	
Elfving et al. (2021)[64]	proprietary aminoresin	Resin with matrix of polystyrene	Primary-amine groups	N.A.	Cyclic (TVSA)	P.B.	22 cycles		• Aminoresin showed 13% capacity loss at 100 °C with air purge, 6% loss at 60 °C (but lower working capacity due to incomplete desorption), and 8% loss in closed TVSA at 100 °C. • Cause of decline under TVSA with closed inlet (oxidative vs. thermal) remained unclear.
							Compressed air (D) 25 °C 1000 mL/min	Compressed air 100 °C	
							23 cycles		
							Compressed air (D) 25 °C 1000 mL/min	Compressed air 60 °C	
					Cyclic (Closed TVSA)		23 cycles		
							Compressed air (D) 25 °C 1000 mL/min	N_2 100 °C	
Gebald et al. (2013)[44]	AEAPDMS-NFC	Nanofibrillated cellulose	AEAPDMS (grafting)	5.9 $mmol_N/g$	C.E.	P.B.	20% O_2/80% N_2 (H) 90 °C 200 mL/min (15 h)		• 30% capacity reduction due to oxidative degradation.
					Cyclic (TVSA)		100 cycles		• About 5% capacity reduction after 100 cycles.
							Ambient air 400−530 ppm CO_2 30 °C 10 L/min RH = 60% (150 min)	90 °C 30 mbar (45 min)	

Reference	Adsorbent	Support material	Active Component	Loading (wt%)	Mode of Experiment		Oxidative stability		Remarks
							Adsorption	Regeneration	
Goeppert et al. (2014)[111]	FS-PEI-33	Aerosil 380 (hydrophilic) fumed silica	bPEI (Mw 25000) (impregnation)	33	Cyclic (TSA)	P.B.	4 cycles		• Stable capture capacity for both samples.
							Air with 400–420 ppm CO_2 (D) 25 °C 335 mL/min	Air 85 °C 335 mL/min	
	FS-PEI-50			50					
Goeppert et al. (2019)[15]	TEPA/50S	Sipernat 50S silica	TEPA (impregnation)	50	C.E.	G.A.	Mass loss observed in oxidative treatment under air containing 21 % O_2 in N_2 at 100 °C for 20 h following by CO2 adsorption measurement (under 95% CO_2 in N_2).		• Epoxy-modified sorbents were more stable than sole TEPA- and PEHA-loaded samples. • 35% and 5% mass loss for TEPA/50S and TEPA-PO-1-2/50S, respectively. • Minimal weight loss for LPEI25k. • TEPA/50S faced ≈ 90% capacity loss, whereas TEPA-PO-1-2/50S showed 16% and 18% losses at 55 and 85 °C, respectively; a similar trend was observed for PEHA/50S and PEHA-PO-1-2/50S. • 50% capacity decline TEPA/50S after aging for 3 years (from 3.8 to 1.9 mmol/g. • The capacity loss was greater at higher adsorption temperatures (about 60%).
	TEPA-PO-1-2/50S		TEPA (impregnation) PO-Modified						
	PEHA/50S		PEHA (impregnation)						
	PEHA-PO-1-2/50S		PEHA (impregnation) PO-Modified				After storing samples for 3 years at RT, the capacity of adsorbent was measured at 25, 55, 85 °C (under 95% CO_2 in N_2) (aging or shelf-storing experiments).		
	PEHA-BO-1-2/50S		PEHA (impregnation) BO-Modified						
	LPEI25k/50S		lPEI (Mw 25000) (Impregnation)						
	TEPA-PO-1-2/50S		TEPA (impregnation) PO-Modified		Cyclic (TSA)		15 cycles		• Stable cyclic capacity with final value of about 1.2 and 1.4 $mmol_{CO2}$/g for PEHA-PO-1-2/50S and TEPA-PO-1-2/50Sm respectively.
							Air with 400 ppm CO_2 25 °C 60 mL/min (3 h)	N_2 50 and 60 °C 60 mL/min (30 min)	
	PEHA-PO-1-2/50S		PEHA (impregnation) PO-Modified						
	TEPA-PO-1-2/50S		TEPA (impregnation) PO-Modified			P.B.	45 cycles		• Stable cyclic stability of about 2 mmol/g under humid conditions.
							Air with 1000 ppm CO_2 (H) 25 °C RH = 50% 335 mL/ min (3 h)	Air with 400 ppm CO_2 (H) 50 °C RH = 13% 335 mL/ min (60 min)	
	PEHA-PO-1-2/50S		PEHA (impregnation) PO-Modified				5 cycles		• Stable cyclic stability of about 1.5 and 2.25 mmol/g under dry and humid conditions, respectively.
							Air with 1000 ppm CO_2 (D,H) 25 °C RH = 0 and 50% 335 mL/ min (3 h)	Air with 400 ppm CO_2 (D,H) 50 °C RH = 0 and 13% 335 mL/ min (60 min)	

Reference	Adsorbent	Support material	Active Component	Loading (wt%)	Mode of Experiment		Oxidative stability		Remarks
							Adsorption	Regeneration	
Guta et al. (2023)[27]	45% PEI/γ-Al_2O_3	γ-Al_2O_3	bPEI (Mw 800) (impregnation)	45	C.E.	G.A.	Oxidative degradation carried out using TGA-DSC under O_2 balance N_2, 0.04% CO_2/21% O_2 balance N_2, or 0.04% CO_2 balance N_2 at 70 °C and 1 atm (dry and humid (RH ≈ 43%) conditions) at 100 mL/min for different periods.		• The oxidative degradation was more noticeable after 7 days of exposure under CO_2-free air with about 19% capacity loss. • 2% capacity decrease after 7 days of exposure to 0.04% CO_2 in N_2. • 17% and 80% uptake decline after 3 h and 7 days of exposure to 0.04% CO_2 in air, respectively. • More pronounced effect of CO_2 on oxidative degradation than humidity.
					Cyclic		30 cycles		• The uptake loss was less in the cyclic conditions. • Humidity in cyclic test doubled the uptake loss, attributed to increased water accessibility to the PEI structure and radicals in the CO_2-free states during desorption and ramp down step.
							0.04% CO_2/21% O_2/N_2 (D,H) 30 °C RH=43% (2 h)	N_2 (D,H) 100 °C RH=1.3% (30 min) + temperature was reduced to 70°C under N_2 + Cooling down to 30 °C with 0.04% CO_2/21% O_2/N_2 (30 min)	
Heydari-Gorji and Sayari (2012)[112]	SBA-15PL-600(55)	SBA-15	bPEI (Mn 600) (impregnation)	55	C.E.	G.A.	Exposing samples to carbon-free air (CFair) (dry) and gases with different CO_2/O_2/N_2 mixtures (humid) at 50, 75, 90, 100, and 120 °C for 30 h following by measuring adsorption capacity under same stream at 75 °C.		• By increasing the exposure temperature, the adsorbent further lost its capture capacity, indicating more severe oxidative degradation.
Heydari-Gorji et al. (2011)[37]	pMono	PE-MCM-41 silica	APTMS (grafting)	4.3 $mmol_N/g$	C.E.	G.A. and P.B.	under carbon-free air (CFair) ranging from 70 to 120 °C for 30 h	under carbon-free air (CFair) ranging from 70 to 140 °C for 40 h	• 7.5% capacity loss at 120 °C after 30 h exposure.
	sMono		TMMAPS (grafting)	3.8 $mmol_N/g$					• 5.3% and 32% capacity loss after 30 h exposure at 90 °C at 120 °C, respectively. • In the fixed-bed 86% capacity loss after 40 h exposure at 140 °C.
	tMono		DMAPS (grafting)	N.A.					• The oxidative stability of tMono was confirmed by DRIFT analysis.
	TRI		TRI (grafting)	7.1 $mmol_N/g$					• 5%, 47%, and 94% capacity loss after 30 h at 70, 90, and 120 °C, respectively.

Reference	Adsorbent	Support material	Active Component	Loading (wt%)	Mode of Experiment		Oxidative stability		Remarks
							Adsorption	Regeneration	
Hunt et al. (2024)[69]	Lewatit VPOC1065	Polystyrene-divinylbenzene	Primary amine	N.A.	Cylic (TVSA)	P.B.	180 cycles		• 31.2% capacity decrease was reported.
							Air with 410–420 ppm CO_2 (H) 26 °C RH = 25% 500 mL/min (140 min)	80 °C 100 mbar vacuum (35 min)	
	CA-1	Crosslinked polyamine	Proprietary liquid amine	N.A.			500 cycles		• 14.66 and 28.74% capacity loss at 200 mbar vacuum and atmospheric conditions, respectively.
							Air with 410–420 ppm CO_2 (H) 26 °C RH = 25% 500 mL/min (140 min)	80 °C 500 and 1000 mbar absolute (35 min)	
							500 cycles		• 2.79% capacity decrease was recorded.
							Ambient air with 410–420 ppm CO_2 (H) 26 °C RH = 25% 500 mL/min (140 min)	75 °C 200 mbar absolute (35 min)	
Hunter-Sellars et al. (2024)[113]	PEI/Al_2O_3	γ-Al_2O_3	bPEI (Mw 800) (impregnation)	43	C.E.	G.A.	Oxidative degradation under CO_2-free dry air (21% O_2 in N_2) at 100 °C with a flow rate of 100 mL/min up to 10 days.		• A significant capture capacity was recorded after 5 days of oxidative degradation, with 0.1 mmol/g capacity. • The capture capacity dropped to zero after 10 days of oxidative degradation. • NMR-MOUSE was introduced as a potential method to examine the oxidation level of DAC adsorbents.
Kumar et al. (2020)[20]	Ph-3- ED/SBA-15	SBA-15	Aromatic core with ethylenediamine (impregnation)	50	C.E.	G.A.	Accelerated oxidative treatment at 90 and 110 °C under 21% O_2/He with 90 mL/min for 24 h. Adsorption test under 400 ppm/He at 35 °C for 12 h.		• 65% and 78% capacity decrease at 90 °C for adsorbents prepared with ED and PD, respectively. • Sample prepared with ED exhibited better stability than PD.
	Ph-3-PD/SBA-15		Aromatic core with propylenediamine (impregnation)						

Reference	Adsorbent	Support material	Active Component	Loading (wt%)	Mode of Experiment		Oxidative stability		Remarks
							Adsorption	Regeneration	
Kuwahara et al. (2012)[77]	PEI/SBA-15	SBA-15	bPEI (Mw 800) (impregnation)	30	C.E.	G.A.	TGA mass loss was observed under mixed gas stream of air (30 mL/min) and N_2 (30 mL/min) up to 800 °C.		• Incorporating heteroatoms enhanced the oxidation temperature of PEI-impregnated SBA-15 in the following order: PEI/SBA-15 (181 °C) < PEI/Al-SBA-15 (194 °C) < PEI/Ti-SBA-15 (196 °C) < PEI/Ce-SBA-15 (203 °C) < PEI/Zr-SBA-15 (212 °C).
	PEI/Al-SBA-15	Al-SBA-15							
	PEI/Ti-SBA-15	Ti-SBA-15							
	PEI/Ce-SBA-15	Ce-SBA-15							
	PEI/Zr-SBA-15	Zr-SBA-15							
Meng et al. (2019)[114]	PEI/SiO_2	Silica Sipernat 306	bPEI (Mw 600) (impregnation)	50	C.E.	G.A.	Oxidative degradation under 21% O_2 in N_2 at 30−150 °C for 3−24 h.		• The adsorbent was stable after continuous oxidative treatment below 75 °C for 12 h • A significant capacity loss was observed above 75 °C and reached 90% for treatments above 120 °C. • Color change after oxidative degradation.
					Cyclic (TSA)		50 cycles		• The loss of cyclic capture capacity at 105 °C in the presence of O_2 was 88.5%, whereas in the oxygen-free stream reported as 32.9%.
							15% CO_2/N_2 and 15% CO_2/10% O_2/N_2 30−120 °C (60 min)	N_2 and air 90 °C (30 min)	
Miao et al. (2022)[115]	PEI/SBA-15	SBA-15	bPEI (Mw 800) (impregnation)	50	C.E.	G.A.	Accelerated oxidative treatment under 21% O_2 in N_2 at 70, 80, 90, and 110 °C with flow rate of 100 mL/min for 24 followed by cyclic test		• Acceptable stability for both sorbents below 90 °C, better thermal stability at higher temperatures for PEI-loaded sample. • Capacity loss below 90 °C was attributed to thermal degradation, whereas losses above 90 °C involved both thermal and oxidative deactivation. • Based on the results, a three-phase oxidation mechanism for amine functionalized silica adsorbents
	TEPA/SBA-15		TEPA (impregnation)		Cyclic		10 cycles		
							400 ppm CO_2/N_2 25 °C (D) 100 mL/min (60 min)	N_2 70, 80, 90, and 110 °C 100 mL/min (15 min)	
Min et al. (2018)[116]	PEI/SiO_2	Macroporous silica	bPEI (Mw 1200) (impregnation)	50	C.E.	G.A.	Accelerated oxidative aging under 3% O_2 in N_2 at 110 °C for 24 h.		• The CO_2 working capacity of PEI/SiO_2 dropped by 52% following oxidative treatment, while EB-PEI/SiO_2 experienced a smaller reduction of 23%.
	EB-PEI/SiO_2		bPEI (Mw 1200) (impregnation) functionalized with 1,2-epoxybutane						
	PEI/SiO_2 + 2 wt% TSP	macroporous silica impregnated with TSP chelator	bPEI (Mw 1200) (impregnation)				Oxidative deactivation under 3% O_2, 15% CO_2, 10% H_2O in N_2 balance for 30 days.		• EB-PEI/SiO_2 + 2 wt% TSP experienced less than 10% capacity decrease, whereas PEI/SiO_2 + 2 wt% TSP encountered about 80% capacity loss.
	EB-PEI/SiO_2 + 2 wt% TSP		bPEI (Mw 1200) (impregnation) functionalized with 1,2-epoxybutane						

Reference	Adsorbent	Support material	Active Component	Loading (wt%)	Mode of Experiment		Oxidative stability		Remarks
							Adsorption	Regeneration	
Pang et al. (2017)[14]	TETA	SBA-15 silica	TETA (impregnation)	41	C.E.	G.A.	Bubbling liquid aminopolymers with ultrazero grade air at 110 °C (24 h) followed by impregnation. or Oxidative treatment after aminopolymer/SBA-15 composites preparation ultrazero grade air 110 °C (24 h)		• The PPI-based adsorbents had better oxidative stability than PEI-based material. • Oxidative stability trend: TPTA > PI-den > TETA ≈ EI-den
	EI-den		EI-den (impregnation)	38					
	TPTA		TPTA (impregnation)	41					
	PI-den		PI-den (impregnation)	40					
Pang et al. (2018)[5]	PEI/SBA-15	SBA-15 silica	lPEI (Mn 2500 and 25000) (impregnation)	50	C.E.	G.A.	Ultra-zero grade air (D) 110 °C (24 h)		• lPPI/SBA-15 composites were more stable than lPEI/SBA-15. • lPPI/SBA-15 adsorbents maintained 65–83 % of their CO_2 capacity, whereas PEI/SBA-15 retained 20–40% of capacity.
	PPI/SBA-15		lPPI (Mn 700, 1000, 6700 and 36000) (impregnation)						
Potter et al. (2019)[117]	PEI-SBA	SBA-15	bPEI (Mw 800) (impregnation)	49	C.E.	P.B.	Pretreatment under N_2 at 110 °C 20 mL/min for 1 h Oxidative treatment at 90, 110, and 130 °C under air oxygen at 20 mL/min for 24 h.		• Organic content decrease for both samples at 90 and 110 °C accompanied by increase in pore volume and surface area. • More organic matter loss for MePEI-SBA than PEI-SBA. • Increase in organic content at 130 °C for both samples due to production oxygen-containing components alongside pore volume and surface area decrease.
	MePEI-SBA		Methylated bPEI (Mw 800) (impregnation)	70					
	APS-SBA		APTMS (grafting)	12			Pretreatment under N_2 at 110 °C 20 mL/min for 1 h Oxidative treatment at 130 °C under air oxygen at 20 mL/min for 24 h.		• No significant amine loss or leaching due to strong chemical bond between amine components and the support. • Significant decreases in pore volume and surface area of the samples.
	MAPS-SBA		MAPS (grafting)	16					
	DMAPS-SBA		DMAPS (grafting)	17					
Rosu et al. (2020)[6]	45% LPPI 6700-700	SBA-15	lPPI (blend of polymers with Mn 700 and 6700) (impregnation)	45	Accelerated oxidation + Cyclic (TSA)	G.A.	6 cycles: 10% or 400 ppm CO_2/He (D) 35 °C 90 ml/min (1 h)	6 cycles: He 110 °C (30 min)	• The effect of accelerated oxidation under 400 ppm CO_2 was harsher on LPPI 6700-700 samples.

Reference	Adsorbent	Support material	Active Component	Loading (wt%)	Mode of Experiment		Oxidative stability		Remarks
							Adsorption	Regeneration	
continued Rosu et al. (2020)[6]	45% LPPI-SBA15		lPPI (Mn 700, 6700, and 36000) (impregnation)		Cyclic (TSA)	G.A.	20 cycles 10% CO_2/He or 400 ppm CO_2/He (D) 35 °C 90 mL/min (1 h)	He 90 °C (30 min)	• The extended aging and storing method (impregnated adsorbent or polymer storage) had a trivial effect on adsorbent performance.
Sarazen et al. (2019)[4]	PPI/SBA-15	SBA-15	bPPI (impregnation)	30−40	C.E.	G.A.	Ultrazero grade air 110 °C (12/24 h)		• Adsorbent prepared with polymer synthesized HBr had the best amine efficiency and oxidative stability.
	PEI/SBA-15		bPEI (impregnation)	40					
Srikanth and Chuang (2012)[118]	TS 25/75	Silica	TEPA (impregnation)	25	C.E.	P.B.	Oxidative degradation under air at 100 °C for 12 h.		• Color change to yellow compared to the white color of the fresh samples. • The oxidative stability was in the following order: $TP_{200}S < TP_{600}S < TS$. • TS reached its non-zero CO_2 capture capacity in 10 hours, while the addition of PEG extended the stabilization time to 24 h.
	$TP_{200}S$	TEPA-impregnated silica	PEG (Mw 200) (impregnation)	varying weight ratios of TEPA/PEG/SiO_2					
	$TP_{600}S$		PEG (Mw 600) (impregnation)						
Sujan et al. (2019)[11]	PGA-50/SBA-15	SBA-15	PGA (impregnation)	50	C.E.	G.A.	21% O_2/N_2 (D) 110 °C (24 h)		• The capacity of PGA-50/SBA-15 sample decreased by about 50% and had a trivial mass loss in TGA, while PEI/SBA-15 experienced 90% capacity loss.
	BPEI/SBA-15		bPEI (Mw 800) (impregnation)	55					
Vu et al. (2019)[119]	TEPA10/MF	Mesostructured cellular silica foam	TEPA (impregnation)	10	C.E.	P.B.	Accelerated oxidative degradation under O_2/air/gas mixture at 60−100 °C with flow rate of 40 mL/min for 5, 18, and 42 h followed by CO_2 uptake measurement and characterization.		• Under continuous N_2 at 100 °C for 18 h, 96% of the initial capacity was maintained. • The degradation rate was higher when the oxidation time was increased from 5 h to 18 h and 42 h at 100 °C. • Capture capacity was further reduced, and degradation became more severe with increasing amine load. • Sample loaded with 10% amine did not undergo significant capacity loss. • The capture capacity of adsorbents with 30−70 wt% loading was as low as capacity measured for the bare support. • Temperature increase from 60 °C to 80 and 100 °C amplified oxidative degradation. • Samples with 30–70 wt% TEPA tested under airflow experienced 2–3 times less capacity loss at 100 °C for 18 h compared to pure oxygen.
	TEPA30/MF			30					
	TEPA50/MF			50					
	TEPA60/MF			60					
	TEPA70/MF			70					

Reference	Adsorbent	Support material	Active Component	Loading (wt%)	Mode of Experiment		Oxidative stability		Remarks
							Adsorption	Regeneration	
Vu et al. (2021)[13]	BPEI	Mesostructured cellular silica foam	bPEI (Mn 300, 600, 1200 and 25000) (impregnation)	60	C.E.	P.B.	Oxidative degradation carried out under O_2 stream at 80 and 100 °C (dry and humid conditions) at 40 mL/min for 5−42 following by heating up under N2 at 100 °C at 40 mL/min for 19 h.		• The oxidative stability of BPEI-impregnated samples with different Mw was in this order: BPEI300 < BPEI600 < BPEI1200 < BPEI25000 • The maintained capture capacity of other amine-based adsorbent was as follows: TETA < TEPA < PEHA
	TETA		TETA (impregnation)						
	TEPA		TEPA (impregnation)						
	PEHA		PEHA (impregnation)						
	SPER		SPER (impregnation)						
Wang et al. (2015)[120]	HP2MGL-PEI-50	Polymethacrylate-based HP2MGL (commercial resin)	bPEI (Mw 600) (impregnation)	50	Cyclic (TSA)	P.B.	5 cycles		• 20.5% capacity decrease due to deteriorated active sites.
							5000 ppm CO_2/20.5% O_2/N_2 (D) 25 °C 0.1MPa 50 mL/min	N_2 100 °C 50 mL/min (120 min)	
Yan and Sayari[121]	PEI@Silica	Davisil 365 silica	bPEI (Mw 800) (impregnation)	50	Cyclic	G.A.	5 cycles		• EB and PVA were successful in enhancing the oxidative stability of the supported PEI. • Incorporation of metal in the support had catalyzing effect on oxidative degradation. • Using MS, Ammonia, water, and CO_2 were determined as the main volatile products.
	$PVA_{2/3}$-PEI@Silica		bPEI (Mw 800) (impregnation) + PVA as additive				15% CO_2/N_2 60 °C (D) 100 mL/min (20 min)	N_2 110 °C 100 mL/min (10 min)	
	$EB_{0.37}$- PEI@Silica		bPEI (Mw 800) (impregnation) functionalized with EB						
	PEI@Silica-Fe	Davisil 365 silica doped with Fe	bPEI (Mw 800) (impregnation)						
	$PVA_{2/3}$-PEI@Silica-Fe		bPEI (Mw 800) (impregnation) + PVA as additive						
	$EB_{0.37}$-PEI@Silica-Fe		bPEI (Mw 800) (impregnation) functionalized with EB						

Reference	Adsorbent	Support material	Active Component	Loading (wt%)	Mode of Experiment		Oxidative stability		Remarks
							Adsorption	Regeneration	
Yoo et al. (2020)[34]	L-ethyl	Silica	DI (grafting)	Silane loading 1.25 $mmol_{Si}/g$	Cyclic (TSA)	G.A.	4 cycles 400 ppm CO_2/He 25 °C (3 h)	21% O_2/79% N_2 110 °C (3 h)	• 45% uptake capacity decrease after 12 h.
	APS		APTMS (grafting)	1.1 $mmol_{Si}/g$					• APS shows good stability with no capacity decrease.
	L-propyl		3-(2-aminopropylamino)propyltrimethoxysilane (grafting)	1.28 $mmol_{Si}/g$					• 5% uptake capacity drop after 12 h.
	B-ethyl		N^1-(2-Aminoethyl)-N^1-(3-(triethoxysilyl)-propyl)ethane-1,2-diamine (grafting)	1.03 $mmol_{Si}/g$					• 28% uptake capacity decrease after 12 h.
	B-propyl		N^1-(3-Aminopropyl)-N^1-(3-(triethoxysilyl)propyl)propane-1,3-diamine (grafting)	1.17 $mmol_{Si}/g$					• 11% uptake capacity decrease after 12 h.
Yu et al. (2017)[102]	Lewatit	Ion-exchange resin	aminomethylene (Commercial Adsorbent)	N.A.	C.E.	P.B.	air (D) 50, 60, 70, 80, 100, 120 °C (72 h)		• Significant capacity loss above 80 °C. 10%, 30.2%, 46.7%, and 80.5% decline in capacity at temperatures of 70, 80, 100, and 120 °C, respectively.
							Air + N_2; O_2 12% & 21% 80, 100, 120 °C (72 h)		• Less capacity decrease in lower O_2 concentration. 9%, 42%, and 72% capacity decrease at 80, 100, and 120 °C, respectively, versus 30.2%, 46.7%, and 80.5% reduction in air at the same temperatures.
							12%:42%:46% $O_2/CO_2/N_2$ 100 °C P_{H2O}= 2847 Pa (72 h)		• 30% and 24% uptake capacity losses for dry and wet CO_2-containing gases.

Reference	Adsorbent	Support material	Active Component	Loading (wt%)	Mode of Experiment		Oxidative stability		Remarks
							Adsorption	Regeneration	
Zhang et al. (2015)[103]	FS-LPEI(5000)-47.8	Aerosil® 380 hydrophilic fumed silica	lPEI (Mn 5000) (impregnation)	47.8	C.E.	G.A.	Air (D) 70 and 100 °C (20 h)		• Significant mass and capacity loss under airflow at 100 °C, corresponding to about 93% capacity loss.

Table S3. Summary of studies on the **hydro(thermal) stability** of solid DAC adsorbents, including adsorbent types, experimental conditions, and key findings.

Reference	Adsorbent	Support material	Active Component	Loading	Mode of Experiment		Hydro(thermal) stability	Remarks
Al-Absi et al. (2024)[122]	MSF (Imp)	MSF	bPEI (Mw 800) (impregnation)	64.9	C.E.	Autoclave	Placing adsorbent (≈ 200 mg) in an autoclave filled with distilled water and maintaining in the oven at 110 °C for 3 days	• Bare MSF lost about 50% of its surface area and 25% of its pore volume, while the LPAlSi support exhibited a decrease of less than 15% in both surface area and pore volume. • All MSF-supported samples experienced significant capacity loss due to structural collapse. • The PEI-impregnated sorbents on LPAlSi performed poorly due to polymer leaching. • Both grafted and in-situ polymerized adsorbents on LPAlSi showed increased resistance to hydrothermal degradation, the latter exhibiting the greatest stability.
	MSF (graft)		BPEI (Mw 800) (grafting)	36.3				
	MSF (Poly)		cation ring-opening polymerization of 2-ethyl-2-oxazoline (EtOX) (in-situ polymerization)	57.7				
	LPAlSi (Imp)	Large-pore AlMCM-41 aluminosilicate (LPAlSi)	bPEI (Mw 800) (impregnation)	60				
	LPAlSi (graft)		BPEI (Mw 800) (grafting)	32.2				
	LPAlSi (Poly)		cation ring-opening polymerization of 2-ethyl-2-oxazoline (EtOX) (in-situ polymerization)	48.8				
Barsoum et al. (2024)[123]	SIFSIX-3-Ni	N.A.	N.A.	N.A.	C.E.	Aging in oven	Accelerated humid aging in an oven at 70 °C and RH = 80% for 4 days	• Water caused irreversible structural changes in SIFSIX-3-Ni, blocking CO_2 sites and reducing capture efficiency.
Chaikittisilp et al. (2011)[58]	SynA30	γ-alumina	bPEI (Mw 800) (impregnation)	30	C.E.	Autoclave	Accelerated steam treatment at 105 °C for 24 h in an autoclave	• The capture capacity of PEI-impregnated alumina after steam treatment was decreased by 16.3% and 25.2% under stream containing 10% and 400 ppm CO_2.
	MS25	SBA-15		25				
Darunte et al. (2016)[19]	MIL-101(Cr)-PEI-800	MIL-101(Cr)	BPEI (Mw 800) (impregnation)	1.06 mmol/g	C.E.	G.A.	Fully regenerated at 100 °C with a He flow rate of 100 mL/min in a cell, followed by saturation with He at RH ≈ 32%	• CO_2 adsorption capacity remained unaffected after exposure to 32% RH.
Hammache et al. (2013)[43]	PEI-Si	CARiACT Q-10 silica	bPEI (Mn 423) (impregnation)	46	Cyclic	P.B.	6 cycles: 10 vol % CO_2/He, 60 °C, 100 ml/min (until equilibrium) / 90 vol % H_2O/He, 105 °C + Drying under He at 105 °C	• The utilized silica support did not undergo structural collapse due to steam exposure in both continuous and cyclic tests.
	PEI-Sil-Si		bPEI (Mn 423) and aminopropyltrieth	39.2				

Reference	Adsorbent	Support material	Active Component	Loading	Mode of Experiment		Hydro(thermal) stability		Remarks
continued Hammache et al. (2013)[43]			oxysilane as additive (impregnation)		Cyclic + C.E.		1 cycle		• Only 3% capacity decrease was recorded after direct exposure to steam, exhibiting that the drying step plays a role in capacity decline of samples tested in cyclic approach. • PEI-impregnated and silanated adsorbent lost 12% and 10% capture capacity upon testing for 6 cycles, respectively, caused by reagglomeration of amine groups.
							10 vol % CO_2/He 60 °C 100 ml/min (until equilibrium)	PSA at 60 °C followed by TSA at 105 °C	
							Followed by another cycle		
							10 vol % CO_2/He 60 °C 100 ml/min (until equilibrium)	steam (90 vol% H2O/He) 105 °C (5 h) + Drying under He at 105 °C	
					C.E.		Exposure to steam (90 vol% H_2O/He) at 105 °C for 5 h followed by CO_2 capture measurement in dry conditions		
Jahandar Lashaki et al. (2017)[38]	SBA-15-C	SBA-15	N.A.	N.A.	C.E.	P.B.	Bare SBA-15 steam-treated for 24 h at 120 °C		• 7% in BET surface area decline following steam treatment.
	TRI–SBA-15-0.2		TRI (grafting)	≈ 5.5 $mmol_N/g$	Cyclic		Steam treatment for 48 h		• Slight loss in CO_2 capacity, amine efficiency, and kinetics after 2 steam cycles. • BET surface area decreased by 21–37%, attributed to amine restructuring causing diffusional limitations.
							2 steam regeneration cycles (3 h each) in a fixed bed at 110 °C, followed by adsorption capacity measurements in a TGA with 5% CO_2 at 25, 50, and 75 °C		
Jahandar Lashaki et al. (2022)[39]	Si-MCM-41	Large-pore MCM-41	N.A.	N.A.	C.E.	P.B.	Exposure to steam for 24 h at 120 °C		• Large-pore MCM-41 showed ≈ 5% loss in surface area and pore volume. • Al incorporation reduced losses to ≈ 5% (surface area) and ≈ 3% (pore volume).
	Al-MCM-41	MCM-41 aluminosilicate	N.A.	N.A.					
	Si-MCM-41-y	Large-pore MCM-41	TRI (grafting)	5.48 $mmol_N/g$	Cyclic		Samples underwent a steam regeneration cycle (3 h) in a fixed bed at 110 °C, followed by adsorption capacity measurements in TGA with 5% CO_2 at 25, 50, and 75 °C		• TRI grafting on Al-MCM-41 improved CO_2 capacity, adsorption kinetics, and hydrothermal stability, with smaller BET losses (31–35%) than MCM-41 (36–49%).
	Al-MCM-41-y	MCM-41 aluminosilicate		4.63 $mmol_N/g$					
Kuwahara et al. (2012)[77]	PEI/Zr-SBA-15	Zr-SBA-15	bPEI (Mw 800) (impregnation)	30	C.E.	G.A.	(i.e., 25 °C for 12 h under a flow of water-saturated 10% CO_2 gas)		• No significant phase separation between ZrO_2 and SiO_2. • Porosity decrease was observed for zirconosilicate support.
Lee et al. (2014)[124]	1-en	Mg_2(dobpdc)	ED (grafting)	N.A.	Cyclic (TVSA)	G.A.	20 cycles		• 4% capacity loss was reported.
							15% CO_2/N_2 (D) 40 °C 60 mL/min (until saturation)	Ar 120 °C $<10^{-2}$ kPa 60 mL/min (3 h)	

Reference	Adsorbent	Support material	Active Component	Loading	Mode of Experiment		Hydro(thermal) stability		Remarks
continued Lee et al. (2014)[124]					Cyclic (TSA)		5 cycles		• 6% capacity loss was reported.
							390 ppm CO_2/21% O_2/ balanced N_2 (D) 25 °C 60 mL/min (15 h)	Ar 150 °C $<10^{-2}$ kPa 60 mL/min (2 h)	
							5 cycles		• 4% capacity loss was reported.
							Test sequence: (1) Adsorption 15% CO_2/N_2 (D) 40 °C 60 mL/min (until saturation) (2) 6 min exposure to 100% RH (21 °C) (3) Regeneration Ar 130 °C 60 mL/min (4 h)		
Li et al. (2010)[35]	MCF-PEI	Mesocellular silica foam (MCF)	BPEI (Mw 800) (impregnation)	26.9	C.E.		Treatment under steam/air and steam/nitrogen environments at 90–180 °C following by sample characterization and CO_2 capacity measurement at a TGA device under 10% CO_2 at 45 °C and 110 °C adsorption and regeneration temperature, respectively, for 3 h hours for each step.		• Capacity and apparent mass loss was reported for all amine-functionalized samples caused by collapse of silica support as well as amine degradation. • All adsorbents were oxidatively degraded except for APTMS-grafted sample. • The overall steam stability was in the following order: MCF-PEI > MCF-Mono > MCF-DMA
	MCF-Mono		APTMS (grafting)	14.8					
	MCF-DMA		AEAPTMS (grafting)	24.8					
	MCF-HAS		In-situ polymerization of Aziridine	25.4					
Low et al. (2024)[125]	TIFSIX-3-Ni	N.A.	N.A.	N.A.	C.E.	Volumetric	H_2O adsorption isotherms measurement at 25 °C up to 15%, 48%, and 77% RH levels		• The initial capture capacity at 25 °C and 400 ppm CO_2 (1.11 mmol/g) was maintained at 15% RH, whereas it decreased by about 15% at higher RH levels.
							Expose the samples to a closed environment with RH levels of 75% and 90% at 40 °C for 14 days		• The initial capture capacity (0.88 mmol/g) declined about 42% and 47% at 75% and 90% RH, respectively. It decreased by about 56% after storage in ambient air.
							Stored in open vial for 6 months at average temperature and RH of ≈ 22 °C and 45%		

Reference	Adsorbent	Support material	Active Component	Loading	Mode of Experiment		Hydro(thermal) stability		Remarks
continued Low et al. (2024)[125]					Cyclic (TSA)	G.A.	50 cycles		• TIFSIX-3-Ni showed poor hydro stability under humid DAC conditions (at 40 °C and over 50 cycles), with losses in porosity, crystallinity, and CO_2 capacity, accompanied by color changes.
							Ambient air/He (H) 30 °C varying humidity 190 mL/min/ 10 mL/min (1 h)	Ambient air/He 160 °C varying humidity 190 mL/min/ 10 mL/min (15 min)	
Mahajan et al. (2024)[17]	ED@MOF-74	Mg-MOF-74	ED (grafting)	13.11% N content	Cyclic (TSA)	P.B.	18 cycles		• Stable over 18 dry cycles with 2.7% loss; 74% loss in presence of 2 vol% humidity. • PXRD, EA, FTIR, and TGA revealed amine volatilization above 120 °C and ED stripping/dissolution under humid conditions, leading to water-facilitated amine loss and structural degradation.
							400 ppm CO_2/N_2 (D,H) 25 °C 2 vol% H_2O 200 mL/min (5 h)	N_2 120 °C 200 mL/min (until C = 0)	
Min et al. (2017)[126]	PEI/MacS	Macroporous silica (MacS)	PEI (Mw 1200)	10.5 $mmol_N/g$	C.E.	P.B.	Treated under 100% steam at 120 °C up to 14 days		• MacS exhibited better hydrothermal stability than mesoporous silicas, losing only 13% surface area and 10% capacity when PEI-loaded, linked to thicker walls. • Mesoporous supports suffered > 70% surface area loss and 42–61% capacity decline.
	PEI/MCM-41	MCM-41		10.6 $mmol_N/g$					
	PEI/SBA-15	SBA-15		10.8 $mmol_N/g$					
	PEI/MCF	MCF							
Priyadarshini et al. (2023)[85]	TEPA-impregnated γ-Al_2O_3	γ-Al_2O_3	TEPA (impregnation)	20 wt%	Cyclic (TSA)	P.B.	5 cycles		• Stable cyclic uptake capacity with overall breakthrough and pseudo-equilibrium capacities of 0.72 and 1.6 mmol/g.
							400 ppm CO_2/N_2 (H) –20 °C RH = 70% 50 mL/min	N_2 60 °C 50 mL/min (2 h)	
Sakwa-Novak and Jones (2014)[127]	PEI-impregnated γ-alumina	γ-Al_2O_3	bPEI (Mw 800) (impregnation)	8.4 $mmol_N/g$	C.E.	P.B.	Pretreatment under N_2 at 110 °C followed by continuous steam exposure for 5 min, 90 min, 12 h, and 24 h.		• Boehmite formation at exposure for 90 min and longer. • Boehmite formation did not have any impact on capture capacity decrease.
					Cyclic		18 cycles		
							Pretreatment under N_2 at 110 °C, steam exposure for 5 min followed by partial drying and cooling (to 30 °C) under N_2.		
Sakwa-Novak et al. (2016)[128]	PEI-Functionalized Monolithic Alumina Honeycomb Adsorbent	Monolithic Alumina	bPEI (Mw 800) (impregnation)	30	Cyclic (steam-assisted TSA)	P.B.	5 cycles		• About 20% capacity decrease after first test following by constant performance in the next 4 cycles.
							400 ppm CO_2/N_2 25 °C 12.5 L/min 1 atm	Steam exposure 110–120 °C ≈ 5 g/min + drying under hot N_2 1 L/min	

Reference	Adsorbent	Support material	Active Component	Loading	Mode of Experiment		Hydro(thermal) stability		Remarks
Sandhu et al. (2016)[90]	Si/PEI-40	Grade Q-10 silica	bPEI (Mw 800) (impregnation)	40	Cyclic (TSA)	P.B.	20 cycles		• 9% capture capacity decrease over 20 cycles. • No PEI leaching and alterations in surface morphology and amine functionalities were reported.
							10% CO_2/N_2 (D,H) 75 °C Humid gas containing 2.7% moisture (10 min)	10% N_2/90% H_2O 110 °C (10 min) Followed by N_2 stripping 110 °C (10 min)	
Tompkins and Mokaya (2014)[129]	MCM-41	MCM-41	N.A.	N.A.	C.E.		Heated at 900 °C for 4 h in a tube furnace under water vapor-saturated N_2		• MCM-41 lost ≈ 93% surface area after steam treatment. • Al incorporation via dry grafting improved hydrothermal stability, with Al-MCM-41 showing unchanged XRD patterns before and after treatment.
	Al-MCM-41	aluminosilicate Al-MCM-41							
Yu et al. (2017)[102]	Lewatit	ion-exchange resin	aminomethylene (Commercial Adsorbent)	N.A.	C.E.		Exposed to steam for 48 h		• No significant capacity loss after 48 h steam exposure, attributed to adsorbent's synthesis method and strong support–amine bonding.
Zheng et al. (2024)[130]	K_2CO_3/AC	activated carbon	K_2CO_3 (impregnation)	25.8	Cyclic (MSA)	P.B.	50 cycles		• Around 40% capacity loss with 0.33 mmol/g cyclic capture capacity. • The uptake capacity was recovered by re-impregnating K_2CO_3 on the carrier.
							Air (≈ 450 ppm CO_2) (H) 25 °C RH= 5 % 12 L/min (300 min)	Air (≈ 450 ppm CO_2) (H) 25 °C RH= 90% 12 L/min (300 min)	

List of Abbreviation

ActGO	activated graphene oxide
AEAPDMS	N-(2-aminoethyl)-3-aminopropylmethyldimethoxysilane
APTES	(3-Aminopropyl)triethoxysilane
APTMS	3-(Trimethoxysilyl)propylamine or 3-(aminopropyl)trimethoxysilane
BET	Brunauer–Emmett–Teller
B-ethyl	N^1-(2-Aminoethyl)-N^1-(3-(triethoxysilyl)-propyl)ethane-1,2-diamine
bPEI	branched poly(ethylenimine)
bPPI	branched poly(propylene imine)
B-propyl	N^1-(3-Aminopropyl)-N^1-(3-(triethoxysilyl)propyl)propane-1,3-diamine
C	Outlet carbon dioxide Concentration
C.E.	Continuous exposure experiment
C_0	Inlet carbon dioxide Concentration beginning of the adsorption
CA	cellulose acetate
CO_2	carbon dioxide
CSA	Concentration swing adsorption
D	Dry gas stream
DAC	Direct Air Capture
DETA	diethylenetriamine
DI	N-[3-(trimethoxysilyl)propyl]ethylenediamine or 3-(2-aminoethylamino)propyltrimethoxysilane
DMAPS	(N,N-dimethylaminopropyl)trimethoxysilane
DMEDA	N,N'-Dimethylethylenediamine
DRIFT	diffuse reflectance infrared Fourier transform
DSC	Differential Scanning Calorimetry
e	molar ration
EA	elemental analysis
EB	1,2-epoxybutane
ED	ethylenediamine
EI-den	dendritic PEI
ESI-MS	electrospray ionization mass spectrometry
FT-IR	Fourier-transform infrared spectroscopy
G.A.	Gravimetric analysis
H	Humid gas stream
H_2O	Water
HNTs	halloysite nanotubes
H-SiO_2	hierarchical meso-/macroporous silica structure
lPEI	linear poly(ethylenimine)
lPPI	linear poly(propylene imine)
L-propyl	3-(2-aminopropylamino)propyltrimethoxysilane
MAPS	(N-methylaminopropyl)-trimethoxysilane or (3-methylaminopropyl)trimethoxysilane
MCF	Mesocellular silica foam
MDCM	MOF-derived carbon monoliths
Mn	Number-average molecular weight
MOF	Metal-Organic Framework

MSA	Moisture swing adsorption
MSF	Mesoporous silica foam
Mw	Weight-average molecular weight
NFC	nanofibrillated cellulose
NMR	Nuclear Magnetic Resonance
P.B.	Packed bed experiment
PAA	poly(allylamine)
PAN	polyacrylonitrile
PEG	polyethylene glycol
PEHA	pentaethylenehexamine
PE-MCM-41	pore-expanded MCM-41 silica
PGA	poly(glycidyl amine)
PI-den	dendritic PPI
PMMA	poly(methyl methacrylate)
PO	Propylene oxide
PPG	poly(propylene guanidine)
PVA	polyvinyl alcohol
PXRD	Powder X-ray diffraction
RH	relative humidity
SG	Silica Gel
SPER	spermine
S-TSA	steam-assisted TSA
S-TVSA	steam-assisted Temperature–Vacuum Swing Adsorption
T-BRN	4-(2-aminoethyl)-N-(2-aminoethyl)-N'-[2-[(2-aminoethyl)amino]ethyl]-1,2-ethanediamine
TCSA	Temperature Concentration Swing Adsorption
TEPA	tetraethylenepentamine
T-EPZ	1-[2-[[2-[(2aminoethyl)amino]ethyl]amino]ethyl]-piperazine
TETA	triethylenetetramine
TGA	Thermogravimetric Analysis
T-IPZ	1-(2-aminoethyl)-4-[[(2-aminoethyl)amino]ethyl]piperazine
T-LIN	1,4,7,10,13-pentaazatridecane
TMMAPS	trimethoxy[3-(methylamino)propyl]silane or N-methylaminoproyltrimethoxysilane
TPD	Temperature programmed desorption
TPTA	tripropylenetetramine
TREN	tris(2-aminoethyl)amine
TRI	N1-(3-trimethoxy-silylpropyl)diethylenetriamine or 3-[2-(2-Aminoethylamino)ethylamino]propyltrimethoxysilane or 2-[2-(3-trimethoxysilylpropylamino) ethylamino]ethylamine
TSA	Temperature Swing Adsorption
TSP	Trisodiumphosphate
TVCSA	Temperature–Vacuum Concentration Swing Adsorption
TVSA	Temperature–Vacuum Swing Adsorption
wt%	Weight percentage
XRD	X-ray diffraction
γ-Al_2O_3	γ-alumina

References

(1) Wilfong, W. C.; Srikanth, C. S.; Chuang, S. S. C. In Situ ATR and DRIFTS Studies of the Nature of Adsorbed CO2 on Tetraethylenepentamine Films. *ACS Appl. Mater. Interfaces* **2014**, *6* (16), 13617–13626. https://doi.org/10.1021/am5031006.

(2) Huhe, F.; King, J.; Chuang, S. S. C. Amine-Based Sorbents for CO2 Capture from Air and Flue Gas—a Short Review and Perspective. *Research on Chemical Intermediates*. Springer Science and Business Media B.V. March 1, 2023, pp 791–817. https://doi.org/10.1007/s11164-022-04902-7.

(3) Ahmadian Hosseini, A.; Jahandar Lashaki, M. A Comprehensive Evaluation of Amine-Impregnated Silica Materials for Direct Air Capture of Carbon Dioxide. *Sep. Purif. Technol.* **2023**, *325*. https://doi.org/10.1016/j.seppur.2023.124580.

(4) Sarazen, M. L.; Sakwa-Novak, M. A.; Ping, E. W.; Jones, C. W. Effect of Different Acid Initiators on Branched Poly(Propylenimine) Synthesis and CO2 Sorption Performance. *ACS Sustain. Chem. Eng.* **2019**, *7* (7), 7338–7345. https://doi.org/10.1021/acssuschemeng.9b00512.

(5) Pang, S. H.; Lively, R. P.; Jones, C. W. Oxidatively-Stable Linear Poly(Propylenimine)-Containing Adsorbents for CO2 Capture from Ultradilute Streams. *ChemSusChem* **2018**, *11* (15), 2628–2637. https://doi.org/10.1002/cssc.201800438.

(6) Rosu, C.; Pang, S. H.; Sujan, A. R.; Sakwa-Novak, M. A.; Ping, E. W.; Jones, C. W. Effect of Extended Aging and Oxidation on Linear Poly(Propylenimine)-Mesoporous Silica Composites for CO2Capture from Simulated Air and Flue Gas Streams. *ACS Appl. Mater. Interfaces* **2020**, *12* (34), 38085–38097. https://doi.org/10.1021/acsami.0c09554.

(7) Park, S. J.; Lee, J. J.; Hoyt, C. B.; Kumar, D. R.; Jones, C. W. Silica Supported Poly(Propylene Guanidine) as a CO2 Sorbent in Simulated Flue Gas and Direct Air Capture. *Adsorption* **2020**, *26* (1), 89–101. https://doi.org/10.1007/s10450-019-00171-w.

(8) Sayari, A.; Heydari-Gorji, A.; Yang, Y. CO2-Induced Degradation of Amine-Containing Adsorbents: Reaction Products and Pathways. *J. Am. Chem. Soc.* **2012**, *134* (33), 13834–13842. https://doi.org/10.1021/ja304888a.

(9) Chaikittisilp, W.; Khunsupat, R.; Chen, T. T.; Jones, C. W. Poly(Allylamine)-Mesoporous Silica Composite Materials for CO 2 Capture from Simulated Flue Gas or Ambient Air. *Ind. Eng. Chem. Res.* **2011**, *50* (24), 14203–14210. https://doi.org/10.1021/ie201584t.

(10) Bali, S.; Chen, T. T.; Chaikittisilp, W.; Jones, C. W. Oxidative Stability of Amino Polymer-Alumina Hybrid Adsorbents for Carbon Dioxide Capture. *Energy and Fuels* **2013**, *27* (3), 1547–1554. https://doi.org/10.1021/ef4001067.

(11) Sujan, A. R.; Kumar, D. R.; Sakwa-Novak, M.; Ping, E. W.; Hu, B.; Park, S. J.; Jones, C. W. Poly(Glycidyl Amine)-Loaded SBA-15 Sorbents for CO2 Capture from Dilute and Ultradilute Gas Mixtures. *ACS Appl. Polym. Mater.* **2019**, *1* (11), 3137–3147. https://doi.org/10.1021/acsapm.9b00788.

(12) Kumar, R.; Bandyopadhyay, M.; Pandey, M.; Tsunoji, N. Amine-Impregnated Nanoarchitectonics of Mesoporous Silica for Capturing Dry and Humid 400 Ppm Carbon Dioxide: A Comparative Study. *Microporous and Mesoporous Materials* **2022**, *338*. https://doi.org/10.1016/j.micromeso.2022.111956.

(13) Vu, Q. T.; Yamada, H.; Yogo, K. Effects of Amine Structures on Oxidative Degradation of Amine-Functionalized Adsorbents for CO2Capture. *Ind. Eng. Chem. Res.* **2021**, *60* (13), 4942–4950. https://doi.org/10.1021/acs.iecr.0c05694.

(14) Pang, S. H.; Lee, L. C.; Sakwa-Novak, M. A.; Lively, R. P.; Jones, C. W. Design of Aminopolymer Structure to Enhance Performance and Stability of CO2 Sorbents: Poly(Propylenimine) vs Poly(Ethylenimine). *J. Am. Chem. Soc.* **2017**, *139* (10), 3627–3630. https://doi.org/10.1021/jacs.7b00235.

(15) Goeppert, A.; Zhang, H.; Sen, R.; Dang, H.; Prakash, G. K. S. Oxidation-Resistant, Cost-Effective Epoxide-Modified Polyamine Adsorbents for CO2 Capture from Various Sources Including Air. *ChemSusChem* **2019**, *12* (8), 1712–1723. https://doi.org/10.1002/cssc.201802978.

(16) Liu, Z.; Teng, Y.; Zhang, K.; Chen, H.; Yang, Y. CO2 Adsorption Performance of Different Amine-Based Siliceous MCM-41 Materials. *Journal of Energy Chemistry* **2015**, *24* (3), 322–330. https://doi.org/10.1016/S2095-4956(15)60318-7.

(17) Mahajan, S.; Elfving, J.; Lahtinen, M. Evaluating the Viability of Ethylenediamine-Functionalized Mg-MOF-74 in Direct Air Capture: The Challenges of Stability and Slow Adsorption Rate. *J. Environ. Chem. Eng.* **2024**, *12* (2). https://doi.org/10.1016/j.jece.2024.112193.

(18) Bose, S.; Sengupta, D.; Malliakas, C. D.; Idrees, K. B.; Xie, H.; Wang, X.; Barsoum, M. L.; Barker, N. M.; Dravid, V. P.; Islamoglu, T.; Farha, O. K. Suitability of a Diamine Functionalized Metal-Organic Framework for Direct Air Capture. *Chem. Sci.* **2023**, *14* (35), 9380–9388. https://doi.org/10.1039/d3sc02554c.

(19) Darunte, L. A.; Oetomo, A. D.; Walton, K. S.; Sholl, D. S.; Jones, C. W. Direct Air Capture of CO2 Using Amine Functionalized MIL-101(Cr). *ACS Sustain. Chem. Eng.* **2016**, *4* (10), 5761–5768. https://doi.org/10.1021/acssuschemeng.6b01692.

(20) Kumar, D. R.; Rosu, C.; Sujan, A. R.; Sakwa-Novak, M. A.; Ping, E. W.; Jones, C. W. Alkyl-Aryl Amine-Rich Molecules for CO2 Removal via Direct Air Capture. *ACS Sustain. Chem. Eng.* **2020**, *8* (29), 10971–10982. https://doi.org/10.1021/acssuschemeng.0c03706.

(21) Hack, J.; Maeda, N.; Meier, D. M. Review on CO2 Capture Using Amine-Functionalized Materials. *ACS Omega*. American Chemical Society November 8, 2022, pp 39520–39530. https://doi.org/10.1021/acsomega.2c03385.

(22) Hack, J.; Frazzetto, S.; Evers, L.; Maeda, N.; Meier, D. M. Branched Versus Linear Structure: Lowering the CO2 Desorption Temperature of Polyethylenimine-Functionalized Silica Adsorbents. *Energies (Basel).* **2022**, *15* (3). https://doi.org/10.3390/en15031075.

(23) Wang, X.; Song, C. Temperature-Programmed Desorption of CO2 from Polyethylenimine-Loaded SBA-15 as Molecular Basket Sorbents. In *Catalysis Today*; 2012; Vol. 194, pp 44–52. https://doi.org/10.1016/j.cattod.2012.08.008.

(24) Zhu, X.; Xie, W.; Wu, J.; Miao, Y.; Xiang, C.; Chen, C.; Ge, B.; Gan, Z.; Yang, F.; Zhang, M.; O'Hare, D.; Li, J.; Ge, T.; Wang, R. Recent Advances in Direct Air Capture by Adsorption. *Chemical Society Reviews*. Royal Society of Chemistry July 11, 2022, pp 6574–6651. https://doi.org/10.1039/d1cs00970b.

(25) Hahn, M. W.; Jelic, J.; Berger, E.; Reuter, K.; Jentys, A.; Lercher, J. A. Role of Amine Functionality for CO2 Chemisorption on Silica. *Journal of Physical Chemistry B* **2016**, *120* (8), 1988–1995. https://doi.org/10.1021/acs.jpcb.5b10012.

(26) Li, K.; Jiang, J.; Yan, F.; Tian, S.; Chen, X. The Influence of Polyethyleneimine Type and Molecular Weight on the CO2 Capture Performance of PEI-Nano Silica Adsorbents. *Appl. Energy* **2014**, *136*, 750–755. https://doi.org/10.1016/j.apenergy.2014.09.057.

(27) Guta, Y. A.; Carneiro, J.; Li, S.; Innocenti, G.; Pang, S. H.; Sakwa-Novak, M. A.; Sievers, C.; Jones, C. W. Contributions of CO2, O2, and H2O to the Oxidative Stability of Solid Amine Direct Air Capture Sorbents at Intermediate Temperature. *ACS Appl. Mater. Interfaces* **2023**, *15* (40), 46790–46802. https://doi.org/10.1021/acsami.3c08140.

(28) Harpe, V.; Petersen, H.; Li, Y.; Kissel, T. Characterization of Commercially Available and Synthesized Polyethylenimines for Gene Delivery. *Journal of Controlled Release* **2000**, *69*, 309–322.

(29) Hicks, J. C.; Drese, J. H.; Fauth, D. J.; Gray, M. L.; Qi, G.; Jones, C. W. Designing Adsorbents for CO2 Capture from Flue Gas-Hyperbranched Aminosilicas Capable of Capturing CO2 Reversibly. *J. Am. Chem. Soc.* **2008**, *130* (10), 2902–2903. https://doi.org/10.1021/ja077795v.

(30) Chen, C.; Zhang, S.; Row, K. H.; Ahn, W. S. Amine–Silica Composites for CO2 Capture: A Short Review. *Journal of Energy Chemistry*. Elsevier B.V. November 1, 2017, pp 868–880. https://doi.org/10.1016/j.jechem.2017.07.001.

(31) Wamba, A. G. N.; Kofa, G. P.; Koungou, S. N.; Thue, P. S.; Lima, E. C.; Dos Reis, G. S.; Kayem, J. G. Grafting of Amine Functional Group on Silicate Based Material as Adsorbent for Water Purification: A Short Review. *Journal of Environmental Chemical Engineering*. Elsevier Ltd April 1, 2018, pp 3192–3203. https://doi.org/10.1016/j.jece.2018.04.062.

(32) Calleja, G.; Sanz, R.; Arencibia, A.; Sanz-Pérez, E. S. Influence of Drying Conditions on Amine-Functionalized SBA-15 as Adsorbent of CO2. In *Topics in Catalysis*; 2011; Vol. 54, pp 135–145. https://doi.org/10.1007/s11244-011-9652-7.

(33) Bollini, P.; Choi, S.; Drese, J. H.; Jones, C. W. Oxidative Degradation of Aminosilica Adsorbents Relevant to Postcombustion CO2 Capture. *Energy and Fuels* **2011**, *25* (5), 2416–2425. https://doi.org/10.1021/ef200140z.

(34) Yoo, C. J.; Park, S. J.; Jones, C. W. CO2 Adsorption and Oxidative Degradation of Silica-Supported Branched and Linear Aminosilanes. *Ind. Eng. Chem. Res.* **2020**, *59* (15), 7061–7071. https://doi.org/10.1021/acs.iecr.9b04205.

(35) Li, W.; Bollini, P.; Didas, S. A.; Choi, S.; Drese, J. H.; Jones, C. W. Structural Changes of Silica Mesocellular Foam Supported Amine-Functionalized CO2 Adsorbents upon Exposure to Steam. *ACS Appl. Mater. Interfaces* **2010**, *2* (11), 3363–3372. https://doi.org/10.1021/am100786z.

(36) Ahmadalinezhad, A.; Tailor, R.; Sayari, A. Molecular-Level Insights into the Oxidative Degradation of Grafted Amines. *Chemistry - A European Journal* **2013**, *19* (32), 10543–10550. https://doi.org/10.1002/chem.201300864.

(37) Heydari-Gorji, A.; Belmabkhout, Y.; Sayari, A. Degradation of Amine-Supported CO2 Adsorbents in the Presence of Oxygen-Containing Gases. *Microporous and Mesoporous Materials* **2011**, *145* (1–3), 146–149. https://doi.org/10.1016/j.micromeso.2011.05.010.

(38) Jahandar Lashaki, M.; Ziaei-Azad, H.; Sayari, A. Insights into the Hydrothermal Stability of Triamine-Functionalized SBA-15 Silica for CO2 Adsorption. *ChemSusChem* **2017**, *10* (20), 4037–4045. https://doi.org/10.1002/cssc.201701439.

(39) Jahandar Lashaki, M.; Ziaei-Azad, H.; Sayari, A. Unprecedented Improvement of the Hydrothermal Stability of Amine-Grafted MCM-41 Silica for CO2 Capture via Aluminum Incorporation. *Chemical Engineering Journal* **2022**, *450*. https://doi.org/10.1016/j.cej.2022.138393.

(40) Jung, H.; Lee, C. H.; Jeon, S.; Jo, D. H.; Huh, J.; Kim, S. H. Effect of Amine Double-Functionalization on CO2 Adsorption Behaviors of Silica Gel-Supported Adsorbents. *Adsorption* **2016**, *22* (8), 1137–1146. https://doi.org/10.1007/s10450-016-9837-2.

(41) Sayari, A.; Belmabkhout, Y. Stabilization of Amine-Containing CO2 Adsorbents: Dramatic Effect of Water Vapor. *J. Am. Chem. Soc.* **2010**, *132* (18), 6312–6314. https://doi.org/10.1021/ja1013773.

(42) Sayari, A.; Belmabkhout, Y.; Da'Na, E. CO2 Deactivation of Supported Amines: Does the Nature of Amine Matter? *Langmuir* **2012**, *28* (9), 4241–4247. https://doi.org/10.1021/la204667v.

(43) Hammache, S.; Hoffman, J. S.; Gray, M. L.; Fauth, D. J.; Howard, B. H.; Pennline, H. W. Comprehensive Study of the Impact of Steam on Polyethyleneimine on Silica for CO2 Capture. *Energy and Fuels* **2013**, *27* (11), 6899–6905. https://doi.org/10.1021/ef401562w.

(44) Gebald, C.; Wurzbacher, J. A.; Tingaut, P.; Steinfeld, A. Stability of Amine-Functionalized Cellulose during Temperature-Vacuum-Swing Cycling for CO2 Capture from Air. *Environ. Sci. Technol.* **2013**, *47* (17), 10063–10070. https://doi.org/10.1021/es401731p.

(45) Didas, S. A.; Zhu, R.; Brunelli, N. A.; Sholl, D. S.; Jones, C. W. Thermal, Oxidative and CO2 Induced Degradation of Primary Amines Used for CO2 Capture: Effect of Alkyl Linker on Stability. *Journal of Physical Chemistry C* **2014**, *118* (23), 12302–12311. https://doi.org/10.1021/jp5025137.

(46) Gleede, T.; Reisman, L.; Rieger, E.; Mbarushimana, P. C.; Rupar, P. A.; Wurm, F. R. Aziridines and Azetidines: Building Blocks for Polyamines by Anionic and Cationic Ring-Opening Polymerization. *Polymer Chemistry*. Royal Society of Chemistry June 28, 2019, pp 3257–3283. https://doi.org/10.1039/c9py00278b.

(47) McDonald, T. M.; Mason, J. A.; Kong, X.; Bloch, E. D.; Gygi, D.; Dani, A.; Crocellà, V.; Giordanino, F.; Odoh, S. O.; Drisdell, W. S.; Vlaisavljevich, B.; Dzubak, A. L.; Poloni, R.; Schnell, S. K.; Planas, N.; Lee, K.; Pascal, T.; Wan, L. F.; Prendergast, D.; Neaton, J. B.; Smit, B.; Kortright, J. B.; Gagliardi, L.; Bordiga, S.; Reimer, J. A.; Long, J. R. Cooperative Insertion of CO2 in Diamine-Appended Metal-Organic Frameworks. *Nature* **2015**, *519* (7543), 303–308. https://doi.org/10.1038/nature14327.

(48) Jo, H.; Lee, W. R.; Kim, N. W.; Jung, H.; Lim, K. S.; Kim, J. E.; Kang, D. W.; Lee, H.; Hiremath, V.; Seo, J. G.; Jin, H.; Moon, D.; Han, S. S.; Hong, C. S. Fine-Tuning of the Carbon Dioxide Capture Capability of Diamine-Grafted Metal–Organic Framework Adsorbents Through Amine Functionalization. *ChemSusChem* **2017**, *10* (3), 541–550. https://doi.org/10.1002/cssc.201601203.

(49) Lee, W. R.; Kim, J. E.; Lee, S. J.; Kang, M.; Kang, D. W.; Lee, H. Y.; Hiremath, V.; Seo, J. G.; Jin, H.; Moon, D.; Cho, M.; Jung, Y.; Hong, C. S. Diamine-Functionalization of a Metal–Organic Framework Adsorbent for Superb Carbon Dioxide Adsorption and Desorption Properties. *ChemSusChem* **2018**, *11* (10), 1694–1707. https://doi.org/10.1002/cssc.201800363.

(50) Siegelman, R. L.; Milner, P. J.; Forse, A. C.; Lee, J. H.; Colwell, K. A.; Neaton, J. B.; Reimer, J. A.; Weston, S. C.; Long, J. R. Water Enables Efficient CO2 Capture from Natural Gas Flue Emissions in an Oxidation-Resistant Diamine-Appended Metal-Organic Framework. *J. Am. Chem. Soc.* **2019**, *141* (33), 13171–13186. https://doi.org/10.1021/jacs.9b05567.

(51) Xiong, S.; Sterling, A. J.; Tkachenko, N. V.; Reyes, R. D.; Tsai, H.; Lee, J.; Chen, Y.; Wang, Y.; Dods, M. N.; Lu, D.; Zhu, Z.; Börgel, J.; Kim, J. W.; Schmeiser, A. J.; Meng, J.; Furukawa, H.; Peters, A. W.; McCloskey, B. D.; Reimer, J. A.; Weston, S. C.; Head-Gordon, M.; Long, J. R. Mechanistic Studies of Oxidative Degradation in Diamine-Appended Metal-Organic Frameworks Exhibiting Cooperative CO2 Capture. *J. Am. Chem. Soc.* **2025**. https://doi.org/10.1021/jacs.5c07551.

(52) Abhilash, K. A. S.; Deepthi, T.; Sadhana, R. A.; Benny, K. G. Functionalized Polysilsesquioxane-Based Hybrid Silica Solid Amine Sorbents for the Regenerative Removal of CO2 from Air. *ACS Appl. Mater. Interfaces* **2015**, *7* (32), 17969–17976. https://doi.org/10.1021/acsami.5b04674.

(53) Alesi, W. R.; Kitchin, J. R. Evaluation of a Primary Amine-Functionalized Ion-Exchange Resin for CO2 Capture. *Ind. Eng. Chem. Res.* **2012**, *51* (19), 6907–6915. https://doi.org/10.1021/ie300452c.

(54) Anyanwu, J. T.; Wang, Y.; Yang, R. T. Amine-Grafted Silica Gels for CO2 Capture Including Direct Air Capture. *Ind. Eng. Chem. Res.* **2020**, *59* (15), 7072–7079. https://doi.org/10.1021/acs.iecr.9b05228.

(55) Anyanwu, J. T.; Wang, Y.; Yang, R. T. CO2 Capture (Including Direct Air Capture) and Natural Gas Desulfurization of Amine-Grafted Hierarchical Bimodal Silica. *Chemical Engineering Journal* **2022**, *427*. https://doi.org/10.1016/j.cej.2021.131561.

(56) Bali, S.; Sakwa-Novak, M. A.; Jones, C. W. Potassium Incorporated Alumina Based CO2 Capture Sorbents: Comparison with Supported Amine Sorbents under Ultra-Dilute Capture Conditions. *Colloids Surf. A Physicochem. Eng. Asp.* **2015**, *486*, 78–85. https://doi.org/10.1016/j.colsurfa.2015.09.020.

(57) Cai, H.; Bao, F.; Gao, J.; Chen, T.; Wang, S.; Ma, R. Preparation and Characterization of Novel Carbon Dioxide Adsorbents Based on Polyethylenimine-Modified Halloysite Nanotubes. *Environmental Technology (United Kingdom)* **2015**, *36* (10), 1273–1280. https://doi.org/10.1080/09593330.2014.984772.

(58) Chaikittisilp, W.; Kim, H. J.; Jones, C. W. Mesoporous Alumina-Supported Amines as Potential Steam-Stable Adsorbents for Capturing CO2 from Simulated Flue Gas and Ambient Air. *Energy and Fuels* **2011**, *25* (11), 5528–5537. https://doi.org/10.1021/ef201224v.

(59) Chao, K. J.; Klinthong, W.; Tan, C. S. CO2 Adsorption Ability and Thermal Stability of Amines Supported on Mesoporous Silica SBA-15 and Fumed Silica. *Journal of the Chinese Chemical Society* **2013**, *60* (7), 735–744. https://doi.org/10.1002/jccs.201200507.

(60) Chen, Z.; Deng, S.; Wei, H.; Wang, B.; Huang, J.; Yu, G. Polyethylenimine-Impregnated Resin for High CO2 Adsorption: An Efficient Adsorbent for CO2 Capture from Simulated Flue Gas and Ambient Air. *ACS Appl. Mater. Interfaces* **2013**, *5* (15), 6937–6945. https://doi.org/10.1021/am400661b.

(61) Chen, Y.; Zhu, L.; Wu, J.; Wang, K.; Ge, T. Feasibility and Effectivity of an Amine-Grafted Alumina Adsorbent for Direct Air Capture. *Langmuir* **2024**. https://doi.org/10.1021/acs.langmuir.4c03673.

(62) Choi, S.; Gray, M. L.; Jones, C. W. Amine-Tethered Solid Adsorbents Coupling High Adsorption Capacity and Regenerability for CO2 Capture from Ambient Air. *ChemSusChem* **2011**, *4* (5), 628–635. https://doi.org/10.1002/cssc.201000355.

(63) Choi, S.; Watanabe, T.; Bae, T. H.; Sholl, D. S.; Jones, C. W. Modification of the Mg/DOBDC MOF with Amines to Enhance CO2 Adsorption from Ultradilute Gases. *Journal of Physical Chemistry Letters* **2012**, *3* (9), 1136–1141. https://doi.org/10.1021/jz300328j.

(64) Elfving, J.; Kauppinen, J.; Jegoroff, M.; Ruuskanen, V.; Järvinen, L.; Sainio, T. Experimental Comparison of Regeneration Methods for CO2 Concentration from Air Using Amine-Based Adsorbent. *Chemical Engineering Journal* **2021**, *404*. https://doi.org/10.1016/j.cej.2020.126337.

(65) Gadipelli, S.; Patel, H. A.; Guo, Z. An Ultrahigh Pore Volume Drives Up the Amine Stability and Cyclic CO2 Capacity of a Solid-Amine@Carbon Sorbent. *Advanced Materials* **2015**, *27* (33), 4903–4909. https://doi.org/10.1002/adma.201502047.

(66) Guo, L.; Hu, X.; Hu, G.; Chen, J.; Li, Z.; Dai, W.; Dacosta, H. F. M.; Fan, M. Tetraethylenepentamine Modified Protonated Titanate Nanotubes for CO2 Capture. *Fuel Processing Technology* **2015**, *138*, 663–669. https://doi.org/10.1016/j.fuproc.2015.07.007.

(67) Guo, Y.; Zhao, C.; Sun, J.; Li, W.; Lu, P. Facile Synthesis of Silica Aerogel Supported K2CO3 Sorbents with Enhanced CO2 Capture Capacity for Ultra-Dilute Flue Gas Treatment. *Fuel* **2018**, *215*, 735–743. https://doi.org/10.1016/j.fuel.2017.11.113.

(68) He, L.; Fan, M.; Dutcher, B.; Cui, S.; Shen, X. dong; Kong, Y.; Russell, A. G.; McCurdy, P. Dynamic Separation of Ultradilute CO 2 with a Nanoporous Amine-Based Sorbent. *Chemical Engineering Journal* **2012**, *189–190*, 13–23. https://doi.org/10.1016/j.cej.2012.02.013.

(69) Hunt, R.; Gillbanks, J.; Czapla, J.; Wan, Z.; Karmelich, C.; White, C.; Wood, C. Representative Longevity Testing of Direct Air Capture Materials. *Chemical Engineering Journal* **2024**, *481*. https://doi.org/10.1016/j.cej.2024.148901.

(70) Irani, M.; Gasem, K. A. M.; Dutcher, B.; Fan, M. CO2 Capture Using Nanoporous TiO(OH)2/Tetraethylenepentamine. *Fuel* **2016**, *183*, 601–608. https://doi.org/10.1016/j.fuel.2016.06.129.

(71) Irani, M.; Jacobson, A. T.; Gasem, K. A. M.; Fan, M. Modified Carbon Nanotubes/Tetraethylenepentamine for CO2 Capture. *Fuel* **2017**, *206*, 10–18. https://doi.org/10.1016/j.fuel.2017.05.087.

(72) Keller, L.; Ohs, B.; Lenhart, J.; Abduly, L.; Blanke, P.; Wessling, M. High Capacity Polyethylenimine Impregnated Microtubes Made of Carbon Nanotubes for CO2 Capture. *Carbon N. Y.* **2018**, *126*, 338–345. https://doi.org/10.1016/j.carbon.2017.10.023.

(73) Kong, Y.; Shen, X.; Fan, M.; Yang, M.; Cui, S. Dynamic Capture of Low-Concentration CO2 on Amine Hybrid Silsesquioxane Aerogel. *Chemical Engineering Journal* **2016**, *283*, 1059–1068. https://doi.org/10.1016/j.cej.2015.08.034.

(74) Kong, Y.; Jiang, G.; Wu, Y.; Cui, S.; Shen, X. Amine Hybrid Aerogel for High-Efficiency CO2 Capture: Effect of Amine Loading and CO2 Concentration. *Chemical Engineering Journal* **2016**, *306*, 362–368. https://doi.org/10.1016/j.cej.2016.07.092.

(75) Kulkarni, V.; Panda, D.; Singh, S. K. Direct Air Capture of CO2 over Amine-Modified Hierarchical Silica. *Ind. Eng. Chem. Res.* **2023**, *62* (8), 3800–3811. https://doi.org/10.1021/acs.iecr.2c02268.

(76) Kuwahara, Y.; Kang, D. Y.; Copeland, J. R.; Brunelli, N. A.; Didas, S. A.; Bollini, P.; Sievers, C.; Kamegawa, T.; Yamashita, H.; Jones, C. W. Dramatic Enhancement of CO 2 Uptake by Poly(Ethyleneimine) Using Zirconosilicate Supports. *J. Am. Chem. Soc.* **2012**, *134* (26), 10757–10760. https://doi.org/10.1021/ja303136e.

(77) Kuwahara, Y.; Kang, D. Y.; Copeland, J. R.; Bollini, P.; Sievers, C.; Kamegawa, T.; Yamashita, H.; Jones, C. W. Enhanced CO2 Adsorption over Polymeric Amines Supported on Heteroatom-Incorporated SBA-15 Silica: Impact of Heteroatom Type and Loading on Sorbent Structure and Adsorption Performance. *Chemistry - A European Journal* **2012**, *18* (52), 16649–16664. https://doi.org/10.1002/chem.201203144.

(78) Kwon, H. T.; Sakwa-Novak, M. A.; Pang, S. H.; Sujan, A. R.; Ping, E. W.; Jones, C. W. Aminopolymer-Impregnated Hierarchical Silica Structures: Unexpected Equivalent CO2 Uptake under Simulated Air Capture and Flue Gas Capture Conditions. *Chemistry of Materials* **2019**, *31* (14), 5229–5237. https://doi.org/10.1021/acs.chemmater.9b01474.

(79) Lawson, S.; Griffin, C.; Rapp, K.; Rownaghi, A. A.; Rezaei, F. Amine-Functionalized MIL-101 Monoliths for CO2 Removal from Enclosed Environments. *Energy and Fuels* **2019**, *33* (3), 2399–2407. https://doi.org/10.1021/acs.energyfuels.8b04508.

(80) Liu, S. H.; Hsiao, W. C.; Sie, W. H. Tetraethylenepentamine-Modified Mesoporous Adsorbents for CO2 Capture: Effects of Preparation Methods. In *Adsorption*; 2012; Vol. 18, pp 431–437. https://doi.org/10.1007/s10450-012-9429-8.

(81) Liu, L.; Chen, J.; Tao, L.; Li, H.; Yang, Q. Aminopolymer Confined in Ethane-Silica Nanotubes for CO2 Capture from Ambient Air. *ChemNanoMat* **2020**, *6* (7), 1096–1103. https://doi.org/10.1002/cnma.201900742.

(82) Miao, Y.; He, Z.; Zhu, X.; Izikowitz, D.; Li, J. Operating Temperatures Affect Direct Air Capture of CO2 in Polyamine-Loaded Mesoporous Silica. *Chemical Engineering Journal* **2021**, *426*. https://doi.org/10.1016/j.cej.2021.131875.

(83) Min, Y. J.; Ganesan, A.; Realff, M. J.; Jones, C. W. Direct Air Capture of CO2 Using Poly(Ethyleneimine)-Functionalized Expanded Poly(Tetrafluoroethylene)/Silica Composite Structured Sorbents. *ACS Appl. Mater. Interfaces* **2022**, *14* (36), 40992–41002. https://doi.org/10.1021/acsami.2c11143.

(84) Parvazinia, M.; Garcia, S.; Maroto-Valer, M. CO2 Capture by Ion Exchange Resins as Amine Functionalised Adsorbents. *Chemical Engineering Journal* **2018**, *331*, 335–342. https://doi.org/10.1016/j.cej.2017.08.087.

(85) Priyadarshini, P.; Rim, G.; Rosu, C.; Song, M. G.; Jones, C. W. Direct Air Capture of CO2 Using Amine/Alumina Sorbents at Cold Temperature. *ACS Environmental Au* **2023**, *3* (5), 295–307. https://doi.org/10.1021/acsenvironau.3c00010.

(86) Qi, G.; Wang, Y.; Estevez, L.; Duan, X.; Anako, N.; Park, A. H. A.; Li, W.; Jones, C. W.; Giannelis, E. P. High Efficiency Nanocomposite Sorbents for CO2 Capture Based on Amine-Functionalized Mesoporous Capsules. *Energy Environ. Sci.* **2011**, *4* (2), 444–452. https://doi.org/10.1039/c0ee00213e.

(87) Rao, N.; Wang, M.; Shang, Z.; Hou, Y.; Fan, G.; Li, J. CO2 Adsorption by Amine-Functionalized MCM-41: A Comparison between Impregnation and Grafting Modification Methods. *Energy and Fuels* **2018**, *32* (1), 670–677. https://doi.org/10.1021/acs.energyfuels.7b02906.

(88) Rim, G.; Kong, F.; Song, M.; Rosu, C.; Priyadarshini, P.; Lively, R. P.; Jones, C. W. Sub-Ambient Temperature Direct Air Capture of CO2using Amine-Impregnated MIL-101(Cr) Enables Ambient Temperature CO2Recovery. *JACS Au* **2022**, *2* (2), 380–393. https://doi.org/10.1021/jacsau.1c00414.

(89) Rodríguez-Mosqueda, R.; Rutgers, J.; Bramer, E. A.; Brem, G. Low Temperature Water Vapor Pressure Swing for the Regeneration of Adsorbents for CO2 Enrichment in Greenhouses via Direct Air Capture. *Journal of CO2 Utilization* **2019**, *29*, 65–73. https://doi.org/10.1016/j.jcou.2018.11.010.

(90) Sandhu, N. K.; Pudasainee, D.; Sarkar, P.; Gupta, R. Steam Regeneration of Polyethylenimine-Impregnated Silica Sorbent for Postcombustion CO2 Capture: A Multicyclic Study. *Ind. Eng. Chem. Res.* **2016**, *55* (7), 2210–2220. https://doi.org/10.1021/acs.iecr.5b04741.

(91) Sanz-Pérez, E. S.; Arencibia, A.; Calleja, G.; Sanz, R. Tuning the Textural Properties of HMS Mesoporous Silica. Functionalization towards CO2 Adsorption. *Microporous and Mesoporous Materials* **2018**, *260*, 235–244. https://doi.org/10.1016/j.micromeso.2017.10.038.

(92) Sayari, A.; Liu, Q.; Mishra, P. Enhanced Adsorption Efficiency through Materials Design for Direct Air Capture over Supported Polyethylenimine. *ChemSusChem* **2016**, *9* (19), 2796–2803. https://doi.org/10.1002/cssc.201600834.

(93) Sehaqui, H.; Gálvez, M. E.; Becatinni, V.; Cheng Ng, Y.; Steinfeld, A.; Zimmermann, T.; Tingaut, P. Fast and Reversible Direct CO2 Capture from Air onto All-Polymer Nanofibrillated Cellulose-Polyethylenimine Foams. *Environ. Sci. Technol.* **2015**, *49* (5), 3167–3174. https://doi.org/10.1021/es504396v.

(94) Spinu, D.; Rout, K. R.; Chen, D. Unveiling the Desorption Performance and Thermal Stability of Unmodified Polyamine-Containing CO2 Adsorbents. *Energy and Fuels* **2024**, *38* (14), 13176–13185. https://doi.org/10.1021/acs.energyfuels.4c02091.

(95) Sujan, A. R.; Pang, S. H.; Zhu, G.; Jones, C. W.; Lively, R. P. Direct CO2 Capture from Air Using Poly(Ethylenimine)-Loaded Polymer/Silica Fiber Sorbents. *ACS Sustain. Chem. Eng.* **2019**, *7* (5), 5264–5273. https://doi.org/10.1021/acssuschemeng.8b06203.

(96) Thakkar, H.; Issa, A.; Rownaghi, A. A.; Rezaei, F. CO2 Capture from Air Using Amine-Functionalized Kaolin-Based Zeolites. *Chem. Eng. Technol.* **2017**, *40* (11), 1999–2007. https://doi.org/10.1002/ceat.201700188.

(97) Veselovskaya, J. V.; Derevschikov, V. S.; Shalygin, A. S.; Yatsenko, D. A. K2CO3-Containing Composite Sorbents Based on a ZrO2 Aerogel for Reversible CO2 Capture from Ambient Air. *Microporous and Mesoporous Materials* **2021**, *310*. https://doi.org/10.1016/j.micromeso.2020.110624.

(98) Wang, X.; Ma, X.; Schwartz, V.; Clark, J. C.; Overbury, S. H.; Zhao, S.; Xu, X.; Song, C. A Solid Molecular Basket Sorbent for CO2 Capture from Gas Streams with Low CO2 Concentration under Ambient Conditions. *Physical Chemistry Chemical Physics* **2012**, *14* (4), 1485–1492. https://doi.org/10.1039/c1cp23366a.

(99) Wang, X.; Ma, X.; Song, C.; Locke, D. R.; Siefert, S.; Winans, R. E.; Möllmer, J.; Lange, M.; Möller, A.; Gläser, R. Molecular Basket Sorbents Polyethylenimine–SBA-15 for CO2 Capture from Flue Gas: Characterization and Sorption Properties. *Microporous and Mesoporous Materials* **2013**, *169*, 103–111. https://doi.org/10.1016/j.micromeso.2012.09.023.

(100) Wang, J.; Huang, H.; Wang, M.; Yao, L.; Qiao, W.; Long, D.; Ling, L. Direct Capture of Low-Concentration CO2 on Mesoporous Carbon-Supported Solid Amine Adsorbents at Ambient Temperature. *Ind. Eng. Chem. Res.* **2015**, *54* (19), 5319–5327. https://doi.org/10.1021/acs.iecr.5b01060.

(101) Xu, X.; Myers, M. B.; Versteeg, F. G.; Pejcic, B.; Heath, C.; Wood, C. D. Direct Air Capture (DAC) of CO2using Polyethylenimine (PEI) “Snow”: A Scalable Strategy. *Chemical Communications* **2020**, *56* (52), 7151–7154. https://doi.org/10.1039/d0cc02572k.

(102) Yu, Q.; Delgado, J. D. L. P.; Veneman, R.; Brilman, D. W. F. Stability of a Benzyl Amine Based CO2 Capture Adsorbent in View of Regeneration Strategies. *Ind. Eng. Chem. Res.* **2017**, *56* (12), 3259–3269. https://doi.org/10.1021/acs.iecr.6b04645.

(103) Zhang, H.; Goeppert, A.; Prakash, G. K. S.; Olah, G. Applicability of Linear Polyethylenimine Supported on Nano-Silica for the Adsorption of CO2 from Various Sources Including Dry Air. *RSC Adv.* **2015**, *5* (65), 52550–52562. https://doi.org/10.1039/c5ra05428a.

(104) Zhang, G.; Zhao, P.; Hao, L.; Xu, Y. Amine-Modified SBA-15(P): A Promising Adsorbent for CO2 Capture. *Journal of CO2 Utilization* **2018**, *24*, 22–33. https://doi.org/10.1016/j.jcou.2017.12.006.

(105) Zhang, G.; Zhao, P.; Hao, L.; Xu, Y.; Cheng, H. A Novel Amine Double Functionalized Adsorbent for Carbon Dioxide Capture Using Original Mesoporous Silica Molecular Sieves as Support. *Sep. Purif. Technol.* **2019**, *209*, 516–527. https://doi.org/10.1016/j.seppur.2018.07.074.

(106) Zhang, J.; Zheng, X.; Cao, Y.; Wang, Z.; Kawi, S.; Tan, X. Tetraethylenepentamine-Grafted Polyacrylonitrile-Poly(Methyl Methacrylate) Hollow Fibers for Low Concentration CO2 Capture at Ambient Temperature. *Process Safety and Environmental Protection* **2022**, *157*, 390–396. https://doi.org/10.1016/j.psep.2021.11.027.

(107) Zhao, Y.; Zhou, J.; Fan, L.; Chen, L.; Li, L.; Xu, Z. P.; Qian, G. Indoor CO2 Control through Mesoporous Amine-Functionalized Silica Monoliths. *Ind. Eng. Chem. Res.* **2019**, *58* (42), 19465–19474. https://doi.org/10.1021/acs.iecr.9b03338.

(108) Zhao, M.; Xiao, J.; Gao, W.; Wang, Q. Defect-Rich Mg-Al MMOs Supported TEPA with Enhanced Charge Transfer for Highly Efficient and Stable Direct Air Capture. *Journal of Energy Chemistry* **2022**, *68*, 401–410. https://doi.org/10.1016/j.jechem.2021.12.031.

(109) Ahmadalinezhad, A.; Sayari, A. Oxidative Degradation of Silica-Supported Polyethylenimine for CO2 Adsorption: Insights into the Nature of Deactivated Species. *Physical Chemistry Chemical Physics* **2014**, *16* (4), 1529–1535. https://doi.org/10.1039/c3cp53928h.

(110) Gebald, C.; Wurzbacher, J. A.; Tingaut, P.; Zimmermann, T.; Steinfeld, A. Amine-Based Nanofibrillated Cellulose as Adsorbent for CO 2 Capture from Air. *Environ. Sci. Technol.* **2011**, *45* (20), 9101–9108. https://doi.org/10.1021/es202223p.

(111) Goeppert, A.; Zhang, H.; Czaun, M.; May, R. B.; Prakash, G. K. S.; Olah, G. A.; Narayanan, S. R. Easily Regenerable Solid Adsorbents Based on Polyamines for Carbon Dioxide Capture from the Air. *ChemSusChem* **2014**, *7* (5), 1386–1397. https://doi.org/10.1002/cssc.201301114.

(112) Heydari-Gorji, A.; Sayari, A. Thermal, Oxidative, and CO2-Induced Degradation of Supported Polyethylenimine Adsorbents. *Ind. Eng. Chem. Res.* **2012**, *51* (19), 6887–6894. https://doi.org/10.1021/ie3003446.

(113) Hunter-Sellars, E.; Kerr, J. D.; Eshelman, H. V.; Pollard, Z. A.; Varni, A. J.; Sakwa-Novak, M. A.; Marple, M. A. T.; Pang, S. H. Oxidation of Supported Amines for CO2 Direct Air Capture: Assessing Impact on Physical Properties and Mobility via NMR Relaxometry. *Macromol. Chem. Phys.* **2024**, *225* (14). https://doi.org/10.1002/macp.202400023.

(114) Meng, Y.; Jiang, J.; Aihemaiti, A.; Ju, T.; Gao, Y.; Liu, J.; Han, S. Feasibility of CO2 Capture from O2-Containing Flue Gas Using a Poly(Ethylenimine)-Functionalized Sorbent: Oxidative Stability in Long-Term Operation. *ACS Appl. Mater. Interfaces* **2019**, *11* (37), 33781–33791. https://doi.org/10.1021/acsami.9b08048.

(115) Miao, Y.; Wang, Y.; Zhu, X.; Chen, W.; He, Z.; Yu, L.; Li, J. Minimizing the Effect of Oxygen on Supported Polyamine for Direct Air Capture. *Sep. Purif. Technol.* **2022**, *298*. https://doi.org/10.1016/j.seppur.2022.121583.

(116) Min, K.; Choi, W.; Kim, C.; Choi, M. Oxidation-Stable Amine-Containing Adsorbents for Carbon Dioxide Capture. *Nat. Commun.* **2018**, *9* (1). https://doi.org/10.1038/s41467-018-03123-0.

(117) Potter, M. E.; Cho, K. M.; Lee, J. J.; Jones, C. W. Exploring the Acid Gas Sorption Properties of Oxidatively Degraded Supported Amine Sorbents. *Energy and Fuels* **2019**, *33* (2), 1372–1382. https://doi.org/10.1021/acs.energyfuels.8b03688.

(118) Srikanth, C. S.; Chuang, S. S. C. Spectroscopic Investigation into Oxidative Degradation of Silica-Supported Amine Sorbents for CO2 Capture. *ChemSusChem* **2012**, *5* (8), 1435–1442. https://doi.org/10.1002/cssc.201100662.

(119) Vu, Q. T.; Yamada, H.; Yogo, K. Oxidative Degradation of Tetraethylenepentamine-Impregnated Silica Sorbents for CO2 Capture. *Energy and Fuels* **2019**, *33* (4), 3370–3379. https://doi.org/10.1021/acs.energyfuels.8b04307.

(120) Wang, J.; Wang, M.; Li, W.; Qiao, W.; Long, D.; Ling, L. Application of Polyethylenimine-Impregnated Solid Adsorbents for Direct Capture of Low-Concentration CO2. *AIChE Journal* **2015**, *61* (3), 972–980. https://doi.org/10.1002/aic.14679.

(121) Yan, C.; Sayari, A. Spectroscopic Investigation into the Oxidation of Polyethylenimine for CO2 Capture: Mitigation Strategies and Mechanism. *Chemical Engineering Journal* **2024**, *479*. https://doi.org/10.1016/j.cej.2023.147498.

(122) Al-Absi, A. A.; Benneker, A. M.; Mahinpey, N. Amine Sorbents for Sustainable Direct Air Capture: Long-Term Stability and Extended Aging Study. *Energy and Fuels* **2024**, *38* (10), 8938–8950. https://doi.org/10.1021/acs.energyfuels.4c01328.

(123) Barsoum, M. L.; Hofmann, J.; Xie, H.; Chen, Z.; Vornholt, S. M.; dos Reis, R.; Burns, N.; Kycia, S.; Chapman, K. W.; Dravid, V. P.; Farha, O. K. Probing Structural Transformations and Degradation Mechanisms by Direct Observation in SIFSIX-3-Ni for Direct Air Capture. *J. Am. Chem. Soc.* **2024**, *146* (10), 6557–6565. https://doi.org/10.1021/jacs.3c11503.

(124) Lee, W. R.; Hwang, S. Y.; Ryu, D. W.; Lim, K. S.; Han, S. S.; Moon, D.; Choi, J.; Hong, C. S. Diamine-Functionalized Metal-Organic Framework: Exceptionally High CO2 Capacities from Ambient Air and Flue Gas, Ultrafast CO2 Uptake Rate, and Adsorption Mechanism. *Energy Environ. Sci.* **2014**, *7* (2), 744–751. https://doi.org/10.1039/c3ee42328j.

(125) Low, M. Y. A.; Danaci, D.; Azzan, H.; Jiayi, A. L.; Yong, G. W. S.; Itskou, I.; Petit, C. Physicochemical Properties, Equilibrium Adsorption Performance, Manufacturability, and Stability of TIFSIX-3-Ni for Direct Air Capture of CO2. *Energy and Fuels* **2024**, *38* (13), 11947–11965. https://doi.org/10.1021/acs.energyfuels.4c01368.

(126) Min, K.; Choi, W.; Choi, M. Macroporous Silica with Thick Framework for Steam-Stable and High-Performance Poly(Ethyleneimine)/Silica CO2 Adsorbent. *ChemSusChem* **2017**, *10* (11), 2518–2526. https://doi.org/10.1002/cssc.201700398.

(127) Sakwa-Novak, M. A.; Jones, C. W. Steam Induced Structural Changes of a Poly(Ethylenimine) Impregnated γ-Alumina Sorbent for CO2 Extraction from Ambient Air. *ACS Appl. Mater. Interfaces* **2014**, *6* (12), 9245–9255. https://doi.org/10.1021/am501500q.

(128) Sakwa-Novak, M. A.; Yoo, C. J.; Tan, S.; Rashidi, F.; Jones, C. W. Poly(Ethylenimine)-Functionalized Monolithic Alumina Honeycomb Adsorbents for CO2 Capture from Air. *ChemSusChem* **2016**, *9* (14), 1859–1868. https://doi.org/10.1002/cssc.201600404.

(129) Tompkins, J. T.; Mokaya, R. Steam Stable Mesoporous Silica MCM-41 Stabilized by Trace Amounts of Al. *ACS Appl. Mater. Interfaces* **2014**, *6* (3), 1902–1908. https://doi.org/10.1021/am404911x.

(130) Zheng, S.; Cheng, X.; Zhou, W.; Wang, T.; Zhu, L.; Xiao, H.; Chen, X. K2CO3 on Porous Supports for Moisture-Swing CO2 Capture from Ambient Air. *Asia-Pacific Journal of Chemical Engineering* **2024**, *19* (3). https://doi.org/10.1002/apj.3058.